

---

*According to the van der Waals theory, oil and water shouldn't separate and surfactants shouldn't form membranes, but they do . . . Such behaviors are crucial for life as we know it to exist.*

*—Jacob Israelachvili*

---

## 1

## Intermolecular Forces

In nanoscale systems, multiple chemical interactions are involved. For example, let us consider a dispersion of *nanoparticles*, shown in Figure 1.1. The glass vial in the image holds a liquid in which small solid particles (approximately 80 nm in diameter) are suspended. The nanoparticles shown in Figure 1.1 are composed of silver (Ag), which are known to exhibit special optical properties such as enhanced scattering and absorbance. The nanoparticles remain suspended in the liquid because they are coated with a layer of organic molecules, called polymers. What kinds of chemical interactions occur in this nanoscale system?

First, we can identify the chemical bonds that make up the different states of matter in the system. These include the bonds that hold the Ag atoms together within the core of the nanoparticle. Likewise, we can consider the chemical bonds within each molecule of liquid and any other molecules present in the system. *Interatomic* forces are responsible for the chemical bonds that hold atoms together to form molecules and solids. These include ionic, covalent, and metallic bonds – the so-called “strong” bonds. We will cover the formalization of these bonding models in later chapters. As we will find out, these bonds occur over short distances (a few angstroms) and are often highly directional.

But what about the chemical interactions that allow the nanoparticles to remain suspended in the liquid? What about the interaction between nanoparticles? Or the interaction between a molecule of liquid and a nanoparticle? Or between two molecules of liquid? *Intermolecular* forces are responsible for these “weak” or secondary bonds that occur between molecules, particles, and surfaces. The bonds that result from intermolecular forces lack specificity, stoichiometry, and directionality. These forces can also result in interactions that occur over long distances – much longer than interatomic bond lengths.

As we will see throughout Chapter 1, intermolecular forces play an important role in dictating materials and molecular behavior at the nanoscale. We will cover five different types of intermolecular forces: electrostatic, hydrogen bonding, van der Waals (vdW), hydrophobic, and steric forces. For each of these, we will derive and discuss their universal force laws. We will also discuss the differences between these forces for molecules versus nanoscale objects. Finally, we will develop an understanding of how potential energy diagrams can be used to predict the overall intermolecular interactions between two objects as a function of separation distance.

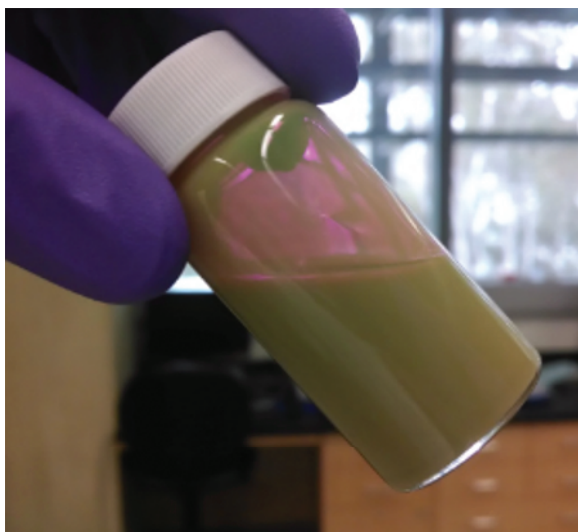


**Figure 1.1** A vial of Ag nanoparticles suspended in liquid.

This knowledge will be applied toward understanding the behavior of nanosystems ranging from atoms and molecules (e.g. DNA and polymers) to particles and other nanomaterials (e.g. liposomes, metal nanoparticles,  $C_{60}$ ).

## 1.1 The Pairwise Potential

Intermolecular forces can lead to attraction or repulsion between atoms, molecules, particles, and surfaces, and contribute significantly to how nanoscale materials and systems behave. These forces are classified as *conservative* forces, meaning that they satisfy the relationship:

$$F = -\frac{dV(r)}{dr} \quad (1.1)$$

where  $F$  is the force,  $V(r)$  is the potential energy of the object, and  $r$  is distance. Because of this relationship, potential energy can be used as a descriptor of whether the force between two objects is attractive or repulsive.

We often consider *pairwise potentials* that describe  $V(r)$  as a function of separation distance to determine attraction or repulsion. For example, two possible pairwise potentials between two spherical particles of radius  $R_s$  are depicted in Figure 1.2.

In a closed system, objects at equilibrium will move into a position that *minimizes the total potential energy*. Thus, in the pairwise potential on the left, the two objects repel each other since  $V(r)$  becomes increasingly positive as the objects approach each other. In the pairwise potential on the right, the two objects attract each other since  $V(r)$  becomes increasingly negative as the objects approach each other.

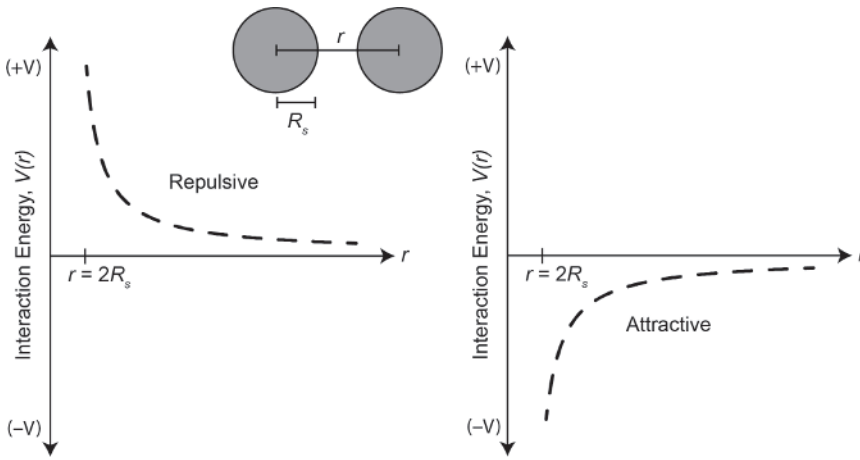


**Figure 1.2** Examples of two pairwise potentials showing repulsive (left) and attractive (right) interactions between approaching spherical particles.

### Worked Example 1.1

**Question:** Consider a volume of liquid-dispersed nanoparticles with separation distance,  $r$ , that behave according to the following pair potential:

$$V(r) = e^{-r/2}$$

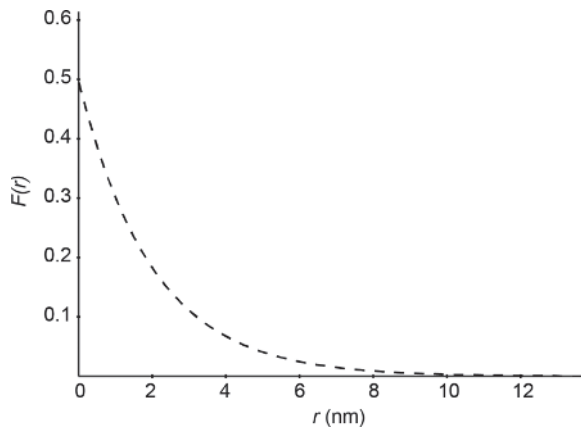
Plot the force curve for two approaching nanoparticles and determine whether you expect the nanoparticles to stay dispersed or aggregate in the liquid at room temperature.

**Answer:** First, we can derive the expression for the force between two approaching quantum dots:

$$F = -\frac{dV(r)}{dr} = -\frac{d}{dr} \left( e^{-r/2} \right) = \frac{1}{2} e^{-r/2}$$

Plotting  $F(r)$  gives Figure 1.3:

**Figure 1.3** Force curve.



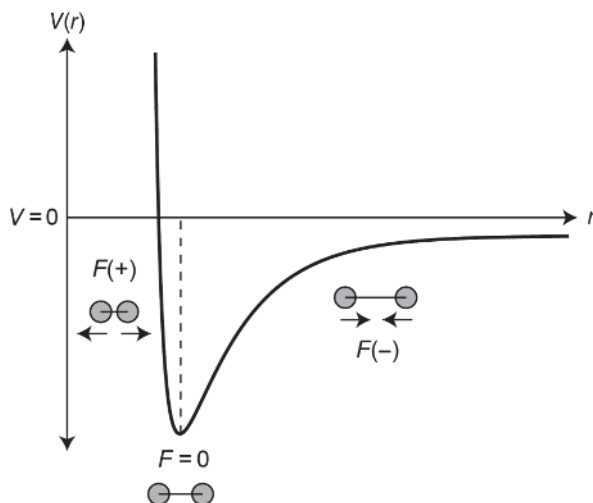


**Figure 1.4** An example of a pair potential where the attractive and repulsive forces cancel each other out, leading to a potential well or energy minimum. The energy minimum in this plot corresponds to the equilibrium of the system.

Since  $F(r)$  is always positive, the force between the nanoparticles is purely repulsive and increases in magnitude as  $r \rightarrow 0$ . Thus, we expect the nanoparticles to repel each other and remain dispersed in the liquid.

In most nanoscale systems, multiple intermolecular interactions contribute to the behavior of a given object. *Equilibrium* is achieved when the net force acting on the object is zero. Consider the pair potential shown in Figure 1.4. There is a strong repulsive potential for small values of  $r$  and a strong attractive potential at large values of  $r$ . At an intermediate value of  $r$ , the attractive and repulsive forces are perfectly balanced. Equilibrium is achieved at this energy minimum, where the slope of the pair-potential curve is equal to zero:

$$F = -\frac{dV(r)}{dr} = 0 \quad (1.2)$$

At equilibrium, a small perturbation of the system will result in the system being restored to the energy minimum. For example, consider what would happen if the two spheres at equilibrium were pulled apart and we increased  $r$  by a small amount: the negative force acting on the spheres would bring the spheres back toward each other and lower  $V(r)$ . Similarly, if we pushed the two spheres closer together and decreased  $r$  by a small amount, the positive force acting on the spheres would pull the spheres away from each other and lower  $V(r)$ . For this reason, the energy minimum shown in Figure 1.4 is also referred to as the *stable* equilibrium or a *potential well*. Note that an equilibrium point corresponding to an energy maximum corresponds to an *unstable* equilibrium.

### Worked Example 1.2

**Question:** Consider two nanoscale objects with a separation distance,  $r$  (in nm), and whose interaction energy is described by the following pair potential:

$$V(r) = -\frac{10}{r} + \frac{1}{r^3}$$

Determine whether or not the two objects can interact and reach a stable equilibrium and the separation distance for which equilibrium occurs.

**Answer:** First, we can recognize that the pair potential consists of an attractive term ( $-10/r$ ) and a repulsive term ( $1/r^3$ ). Equilibrium occurs when the forces associated with these two potential terms cancel each out.

$$\begin{aligned} F &= -\frac{dV(r)}{dr} = 0 \\ &= -\frac{d}{dr} \left( -\frac{10}{r} + \frac{1}{r^3} \right) = -\frac{10}{r^2} + \frac{3}{r^4} \end{aligned}$$

Thus, we can solve for  $r$ :

$$r = (3/10)^{1/2} \approx 0.55 \text{ nm}$$

The objects reach a stable equilibrium at  $r = 0.55 \text{ nm}$  because this corresponds to a minimum in the potential energy diagram.

The pair potential discussed above provides a simple example of how we can use energy and force curves to understand how a nanoscale system will behave (e.g. whether it will be in or out of equilibrium). This will depend entirely on whether an interaction is repulsive or attractive, which in turn is dependent on the strength and distance dependence of each contributing intermolecular interaction. Table 1.1 lists the scaling laws for several different types of intermolecular forces. In the following sections, we will learn about these various intermolecular forces and their corresponding force and energy scaling laws.

## 1.2 Electrostatic Interactions

Electrostatic interactions, which are generated by the electric force between charges, account for a number of interaction geometries found in nanoscale systems. These include:

**Table 1.1** General relationships between interaction geometries and separation distance.

Geometry of interaction	Type of interaction	Distance dependence
Ion-ion	Electrostatic	$1/r$
Ion-dipole	Electrostatic	$1/r^2$
Dipole-dipole	Electrostatic	$1/r^3$
Hydrogen bond	Electrostatic	$1/r^2$
Two atoms	van der Waals	$1/r^6$
Atom-surface	van der Waals	$1/r^3$
Sphere-sphere	van der Waals	$1/r$
Sphere-surface	van der Waals	$1/r$
Surface-surface	van der Waals	$1/r^2$

- ion pairs
- ion–dipole and dipole–dipole interactions
- dative bonds, where a molecule is coordinated to a metal center
- $\pi$ – $\pi$  bonding.

The electric forces in the above interactions are all governed by Coulomb's law, which states that for two bodies with charges  $Q_1$  and  $Q_2$  and separated by a distance,  $r$ , the potential energy of interaction is:

$$V(r) = \frac{Q_1 Q_2}{4\pi\epsilon\epsilon_0 r} \quad (1.3)$$

The corresponding electric force is given by:

$$F = -\frac{dV(r)}{dr} = \frac{-Q_1 Q_2}{4\pi\epsilon\epsilon_0 r^2} \quad (1.4)$$

where the constant  $\epsilon$  is the relative permittivity of the medium surrounding the bodies and  $\epsilon_0$  is the vacuum permittivity. Note that  $Q_1$  and  $Q_2$  can be designated as positive or negative, where like charges are repulsive (resulting in a positive  $V(r)$ ) and unlike charges are attractive (resulting in a negative  $V(r)$ ). *Permittivity* can be thought of as the charge capacitance of a material, where a material with a large  $\epsilon$  value is able to store more of the electric field. A medium with a high permittivity decreases the electrostatic force that is generated from  $Q_1$  and  $Q_2$  since it can more effectively screen the two charged bodies from each other.

### Worked Example 1.3

**Question:** Calculate the interaction potential for a  $\text{Na}^+$  ion and  $\text{Cl}^-$  ion in water with a separation distance of 100 and 0.1 nm. At 20 °C, water has a relative permittivity of  $\epsilon = 80.2$ .

**Answer:** Each ion has a charge of  $+/- e$ . Plugging this into Coulomb's law, we get

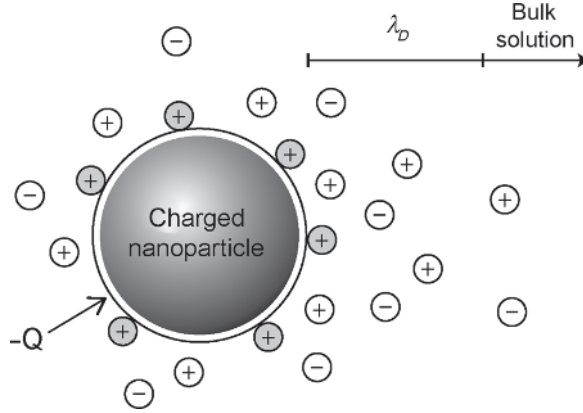
$$\begin{aligned} V(r) &= \frac{Q_1 Q_2}{4\pi\epsilon\epsilon_0 r} = \frac{(+1)(-1)(1.602 \times 10^{-19} \text{ C})^2}{4\pi(80.2) \left(8.85 \times 10^{-12} \frac{\text{C}^2}{\text{J} \cdot \text{m}}\right) r} \\ &= \frac{-2.88 \times 10^{-30} \text{ J} \cdot \text{m}}{r} \\ &= -28.8 \times 10^{-24} \text{ J for } r = 100 \text{ nm} \\ &= -28.8 \times 10^{-21} \text{ J for } r = 0.1 \text{ nm} \end{aligned}$$

It can sometimes be helpful to look at binding energies in units of kJ/mol to compare these values to average bond energies:

$$\begin{aligned} V(r) &= -0.017 \frac{\text{kJ}}{\text{mol}} \text{ for } r = 100 \text{ nm} \\ V(r) &= -17 \frac{\text{kJ}}{\text{mol}} \text{ for } r = 1 \text{ nm} \end{aligned}$$

For comparison, the covalent Cl—Cl bond in  $\text{Cl}_2$  is  $\sim 240$  kJ/mol, over one order of magnitude higher than the binding energy for our electrostatic interaction at 0.1 nm.

**Figure 1.5** Schematic of a spherical particle with a uniform shell of negative charge immersed in an electrolyte solution.



Electric fields that occur in a medium containing free charges (e.g. blood or electrolytes such as a salt solution) undergo electrostatic screening. For example, consider a spherical nanoparticle with surface charge,  $-Q$ , shown in Figure 1.5.

In an electrolyte solution, such as an aqueous solution of NaCl, the ionic charge distribution near the nanoparticle surface becomes much more concentrated compared to the bulk electrolyte. Positively charged ions (e.g.  $\text{Na}^+$ ) are attracted to the negatively charged nanoparticle, causing an increase in ion concentration near the nanoparticle surface. The mobile charges in the electrolyte effectively reduce the overall electric field generated by the charged nanoparticle. The screened electric field decays exponentially according to the following relationship:

$$V(r) = V_0 e^{-r/\lambda_D} \quad (1.5)$$

where the term  $\lambda_D$  is called the Debye length and  $r$  is distance from the nanoparticle surface.  $\lambda_D$  is a characteristic persistence length for the electrostatic effect and can be calculated using the formula:

$$\lambda_D = \sqrt{\frac{\epsilon \epsilon_0 k_B T}{2 N_A e^2 \sum c_i z_i^2}} \quad (1.6)$$

where  $e$  is the elementary charge,  $i$  is the number of different types of ions,  $c$  is the concentration of each ion, and  $z$  is the valence of each ion. An electrolyte such as an aqueous solution of NaCl is considered symmetric (since the number of  $\text{Na}^+$  ions is equal to the number of  $\text{Cl}^-$  ions) and monovalent (since  $z = 1$  for both ions). For a solution of NaCl, the formula for  $\lambda_D$  can be simplified to:

$$\lambda_D(\text{m}) = \sqrt{\frac{\epsilon \epsilon_0 k_B T}{2 N_A e^2 C}} \quad (1.7)$$

where  $C$  is concentration of the dissolved NaCl in molar units (M). Thus, we see that both an increase in the electrolyte concentration and an increase in the ion valence serve to reduce  $\lambda_D$  and more effectively screen electrostatic interactions. Debye lengths for standard electrolyte solutions tend to be between 1 and 100 nm. Because



the dimensions of nanomaterials are on the order of these Debye lengths, electrolyte concentration can have a profound impact on the electrostatic interactions of nanomaterials.

### Worked Example 1.4

**Question:** Calculate  $\lambda_D$  for a nanoparticle dispersed in 1 and 10 mM aqueous solutions of NaCl, and compare the screened electric field,  $V(r)$ , for both cases.

**Answer:** We can plug this electrolyte concentration directly into the formula for  $\lambda_D$ :

$$\begin{aligned}\lambda_D(\text{m}) &= \sqrt{\frac{\epsilon\epsilon_0 k_B T}{2N_A e^2 C}} \\ &= \sqrt{\frac{(80.2) \left(8.85 \times 10^{-12} \frac{\text{C}^2}{\text{J} \cdot \text{m}}\right) \left(1.38 \times 10^{-23} \frac{\text{J}}{\text{K}}\right) (293 \text{ K})}{2(6.02 \times 10^{23})(1.602 \times 10^{-19} \text{ C})^2 \left(\frac{10^{-3} \text{ mol}}{\text{l}}\right) \left(\frac{10^3 \text{ l}}{\text{m}^3}\right)}} \\ &= 9.6 \times 10^{-9} \text{ m} = 9.6 \text{ nm for 1 mM NaCl}\end{aligned}$$

Similarly, we can plug in  $C = 10 \text{ mM}$  to obtain  $\lambda_D = 3.0 \text{ nm}$ . We can compare the electric field potentials for the two concentrations by plotting  $V(r)/V_o$  as a function of distance (Figure 1.6).

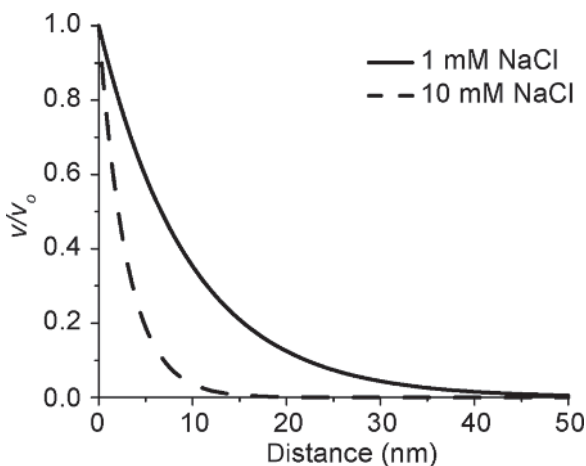


**Figure 1.6** Change in electric field potential for varying electrolyte concentration.

We see that for 10 mM NaCl, nanoparticle charge will be more effectively shielded and the electric field decays much closer to the nanoparticle surface. Note that the Debye length is only dependent on the medium and not the properties of the nanoparticle.

In many nanoscale systems, we must consider the additive effects of multiple pairs of electrostatic interactions. For example, the total binding energy of an *ionic solid* – a material held together almost entirely through electrostatic ionic bonds – can be

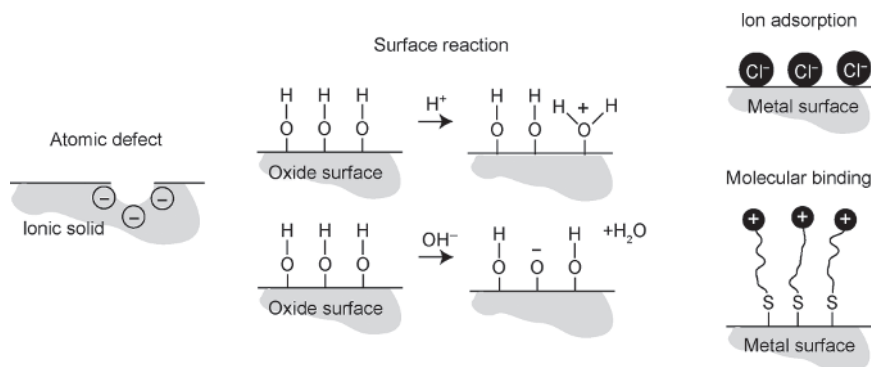


**Figure 1.7** Three examples of how surface charge can be generated on nanostructures.

calculated by summing up all of the ion-pair potentials in the solid. If we wanted to calculate the binding energy in 1 M of table salt (NaCl), we could do so by summing up all ion-pair potentials involving  $\text{Na}^+$  and  $\text{Cl}^-$  ions in the NaCl crystal lattice. Note that this would include both the electrostatic interactions for attractive  $\text{Na}^+/\text{Cl}^-$  pairs and repulsive  $\text{Na}^+/\text{Na}^+$  and  $\text{Cl}^-/\text{Cl}^-$  pairs.

We can also use summation to calculate how electrostatic interactions contribute to the overall binding energy between two charged nanostructures or nanoparticles. However, we must take two major differences into consideration. First, nanostructures are not point charges. Unlike ions such as  $\text{Na}^+$ , nanostructures possess dimensions that approach the Debye length of most media. Second, many nanostructures are not composed of a charged material, but rather possess a net surface charge. Surface charges can arise due to various mechanisms as shown in Figure 1.7, including:

- Atomic defects at the surface
- Adsorption of ions onto the surface
- Adsorption or binding of molecules with functional groups that are charged
- Chemical reactions that occur at the surface (e.g. acid/base reactions).

For nanostructures where surface charges are isotropically (i.e. uniformly) distributed over its surface, it is convenient to describe the surface charge density,  $\sigma$ , given by:

$$\sigma = \frac{\sum q}{A} \quad (1.8)$$

where  $\sum q$  is the total net charge distributed over a surface area,  $A$  (Figure 1.8).

Thus, a nanoparticle that possesses a net surface charge density,  $\sigma$ , can be treated like a uniform shell of charge  $\sum q$ .

### Worked Example 1.5

**Question:** Consider an Au nanoparticle with a diameter,  $d = 30 \text{ nm}$ , that is negatively charged due to adsorbed citrate ions (Figure 1.9).

The citrate ion can be approximated as a sphere with radius  $r = 3.6 \text{ \AA}$ . Estimate the overall net charge,  $Q$ , and the surface charge density,  $\sigma$ , for the Au nanoparticle.

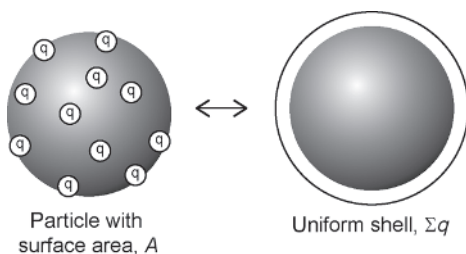


**Figure 1.8** A spherical particle with an isotropic distribution of surface charge.

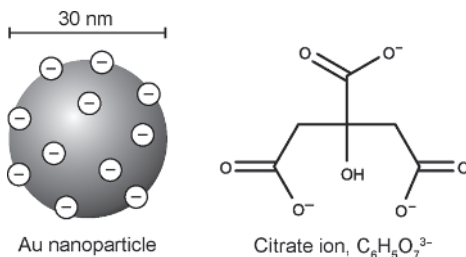


**Figure 1.9** Citrate-coated Au nanoparticle.

**Answer:** Because  $r \ll d$ , we can assume that the citrate ions are uniformly covering the nanoparticle surface. We can estimate the total charge of the nanoparticle by estimating the total number of citrate ions multiplied by the ionic charge. Assuming citrate ions cover the entire surface of the nanoparticle without any consideration of repulsion between citrate ions, we get:

$$Q = \frac{4\pi(15 \text{ nm})^2}{\pi(0.36 \text{ nm})^2} (-3)(1.602 \times 10^{-19} \text{ C}) = -3.3 \times 10^{-15} \text{ C}$$

We can then estimate net surface charge density as:

$$\begin{aligned} \sigma &= \frac{Q}{A} \\ &= \frac{-3.3 \times 10^{-15} \text{ C}}{4\pi(15 \times 10^{-9} \text{ m})^2} = -1.2 \frac{\text{C}}{\text{m}^2} \end{aligned}$$

Now let us consider the case where we would like to calculate the electrostatic-pair potential between a point charge,  $q$ , and a nanoparticle with radius,  $R$ , with a uniform surface charge density,  $\sigma$  (in units of  $\text{C}/\text{m}^2$ ). The separation distance between the center of the nanoparticle and the ion is some distance,  $z$ . Recall that our nanoparticle resembles a hollow shell of charges. We can calculate the total charge potential by adding up the electrostatic interactions for infinitesimally thin, hollow rings of charge with a radius of  $R \sin \theta$  (Figure 1.10).

The distance,  $d$ , between the ion and the shaded ring is given by:

$$d = \sqrt{(R \sin \theta)^2 + (z - R \cos \theta)^2} = \sqrt{z^2 - 2zR \cos \theta + R^2} \quad (1.9)$$

The total charge potential is then given by:

$$V = \frac{q}{4\pi\epsilon\epsilon_0} \cdot 2\sigma \int_0^\pi \frac{\pi R \sin \theta \cdot R d\theta}{d} \quad (1.10)$$

**Figure 1.10** Ion–particle electrostatic interaction.

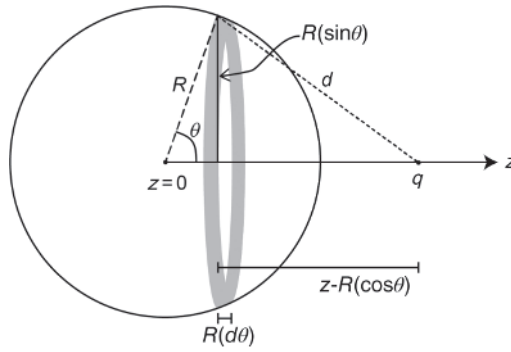
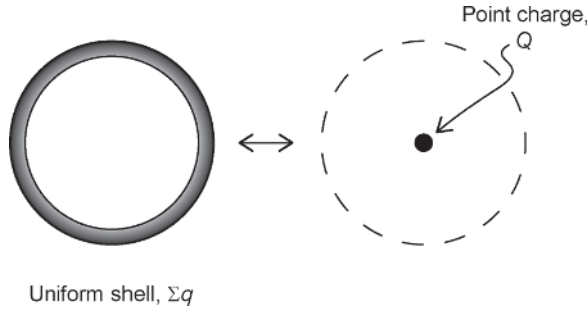


**Figure 1.11** A uniform shell of charge approximated as a point charge.



We can use integration by substitution to help solve the integral:

$$y = d^2 = z^2 - 2zR \cos \theta + R^2$$

$$dy = 2zR \sin \theta d\theta$$

Plugging  $y = d^2$  into our integral, we get:

$$\begin{aligned} V(z) &= \frac{q\sigma}{2\pi\epsilon\epsilon_0} \int_{\theta=0}^{\theta=\pi} \frac{\pi R}{2z} \frac{dy}{y^{\frac{1}{2}}} \\ &= \frac{q\sigma R}{\epsilon\epsilon_0 z} [(z+R) - (z-R)] \\ &= \frac{q\sigma R^2}{\epsilon\epsilon_0 z} = \frac{qQ}{4\pi\epsilon\epsilon_0 z} \end{aligned} \quad (1.11)$$

Thus, we see that for calculating the electrostatic potential between a point charge and a nanoparticle with an even distribution of charge at its surface, the nanoparticle can be treated as a point charge  $Q$  located at the center of the nanoparticle (Figure 1.11).

### Worked Example 1.6

**Question:** Consider the 30 nm Au nanoparticle in water that is negatively charged due to adsorbed citrate ions from the previously worked example. Plot the electrostatic-pair potential between the nanoparticle and a citrate ion as a function of separation distance.

**Answer:** We can treat the charged nanoparticle as a point charge with  $Q = -8.3 \times 10^{-16} \text{ C}$  and the citrate ion as a point charge with  $q = -4.8 \times 10^{-19} \text{ C}$ . Thus, the pair potential can be plotted (Figure 1.12) using Coulomb's law for two ions with a separation distance,  $r$ :

$$\begin{aligned} V(r) &= \frac{Q_1 Q_2}{4\pi\epsilon\epsilon_0 r} = \frac{(-8.3 \times 10^{-16} \text{ C})(-4.8 \times 10^{-19} \text{ C})}{4\pi(80.2) \left(8.85 \times 10^{-12} \frac{\text{C}^2}{\text{J} \cdot \text{m}}\right) r} \\ &= \frac{4.5 \times 10^{-26} \text{ J} \cdot \text{m}^2}{r} = \frac{4.5 \times 10^{-8} \text{ J}}{r(\text{nm})} \end{aligned}$$

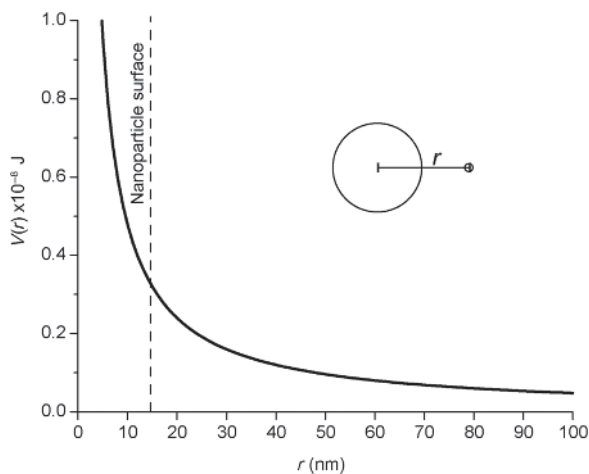


**Figure 1.12** Pair potential for a nanoparticle and citrate ion.

Note that  $r$  is the center-to-center separation distance and that the nanoparticle surface is located at  $r = 15 \text{ nm}$ . Thus, the ion and nanoparticle cannot come closer than a separation distance of  $r = 15 \text{ nm}$ .

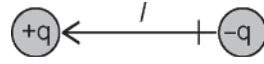
### 1.3 Permanent Dipole Interactions and Hydrogen Bonding

A dipole occurs when there is a separation of charge. In chemical systems, dipole interactions must involve *polar* molecules, which carry no net charge but possess an electric dipole moment. A dipole results when the electronegativity difference between the atoms involved is moderately large.

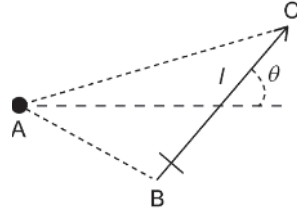
The *dipole moment*,  $\mu$ , for a polar bond is given by:

$$\mu = q \cdot l \quad (1.12)$$

where  $q$  is the charge at either end of the dipole and  $l$  is the length of the bond (Figure 1.13). The moment is typically given in units of Debye (D), where small polar molecules generally exhibit values of  $\mu \approx 1 \text{ D} = 3.336 \times 10^{-30} \text{ C} \cdot \text{m}$ .

**Figure 1.13** Schematic of a dipole.**Worked Example 1.7**

**Question:** Calculate the electrostatic potential generated between an ion with charge,  $Q$ , and a dipole with moment,  $\mu$ , and an arbitrary angle of orientation,  $\theta$  (Figure 1.14).

**Figure 1.14** Ion–dipole interaction.

**Answer:** We can start this problem by considering the electric field generated between the ion and the two opposing ends of the dipole. We can label the locations of the ion and dipole by forming a triangle with corners located at A, B, and C and with the separation distance,  $r$ , bisecting the length of the dipole. This gives the expression:

$$V(r, \theta)_{ion-dip} = \frac{-Qq}{4\pi\epsilon\epsilon_0} \left[ \frac{1}{AB} - \frac{1}{AC} \right]$$

where for  $r \gg l$ :

$$\overline{AB} = \sqrt{\left(r - \frac{l}{2} \cos \theta\right)^2 + \left(\frac{l}{2} \sin \theta\right)^2} \approx r - \frac{l}{2} \cos \theta$$

$$\overline{AC} = \sqrt{\left(r + \frac{l}{2} \cos \theta\right)^2 + \left(\frac{l}{2} \sin \theta\right)^2} \approx r + \frac{l}{2} \cos \theta$$

Plugging this into the expression for  $V(r)$ , we get:

$$\begin{aligned} V(r, \theta)_{ion-dip} &= \frac{-Qq}{4\pi\epsilon\epsilon_0} \left[ \frac{1}{r - \frac{l}{2} \cos \theta} - \frac{1}{r + \frac{l}{2} \cos \theta} \right] \\ &= \frac{-Qq}{4\pi\epsilon\epsilon_0} \left[ \frac{l \cos \theta}{r^2 - \frac{l^2}{4} \cos^2 \theta} \right] \\ &= \frac{-Q(ql) \cos \theta}{4\pi\epsilon\epsilon_0 r^2} \\ V(r, \theta)_{ion-dip} &= \frac{-Q\mu \cos \theta}{4\pi\epsilon\epsilon_0 r^2} \end{aligned} \quad (1.13)$$

In a similar manner to the worked example above, the electrostatic potential between two randomly oriented dipoles with fixed orientations (Figure 1.15) can be calculated:

$$V_{dip-dip} = \frac{-\mu_A \mu_B}{4\pi\epsilon\epsilon_0 r^3} [2 \cos \theta_A \cos \theta_B - \sin \theta_A \sin \theta_B \cos \varphi] \quad (1.14)$$

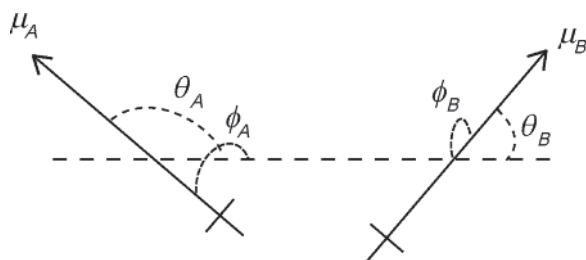


**Figure 1.15** Dipole–dipole interaction.

with the potential energy for two dipoles aligned in head-to-tail configuration (Figure 1.16) given by the simplified expression:

$$V(r) = \frac{-2\mu_A\mu_B}{4\pi\epsilon\epsilon_0r^3} \text{ for } \theta = 0 \quad (1.15)$$

*Hydrogen bonding* is among one of the strongest intermolecular forces and is responsible for a variety of chemical phenomena ranging from the high boiling point of water to the helical structure of DNA. Hydrogen bonding is a specialized electrostatic force that involves a dipole–dipole interaction between two polar bonds (Figure 1.17). One of the dipoles must consist of a bond that contains a H atom that is covalently bound to a small electronegative atom, such as O, N, F, or Cl. This bond is known as the *hydrogen donor*. The other participating dipole serves as the *hydrogen acceptor*. Because the dipole moment of the covalent bond in the H-donor is high, the resulting strong attractive interaction is capable of aligning other polar bonds. The strength of most hydrogen bonds lies between 10 and 40 kJ/mol, which makes them still considerably weaker than the *intramolecular* forces discussed later in Chapter 2. A table of typical hydrogen bonding values is given in Table 1.X.

H donor	H acceptor	H-bond strength (kJ/mol)
F–H	F	161
N–H	N	29
O–H	O	21
N–H	N	13
N–H	O	8

While individual hydrogen bonds are still considered weak bonds, hydrogen bonding can have an additive effect when the bond strengths of multiple hydrogen



**Figure 1.16** Aligned dipoles.

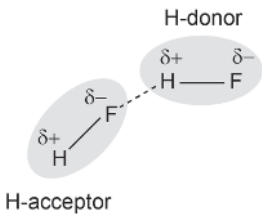


**Figure 1.17** Hydrogen bonding between HF molecules.

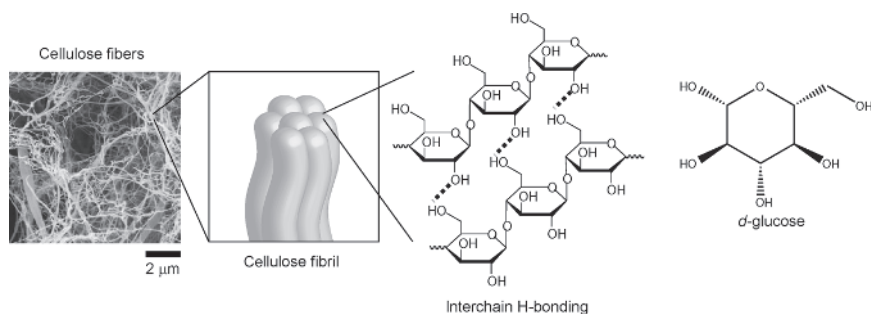


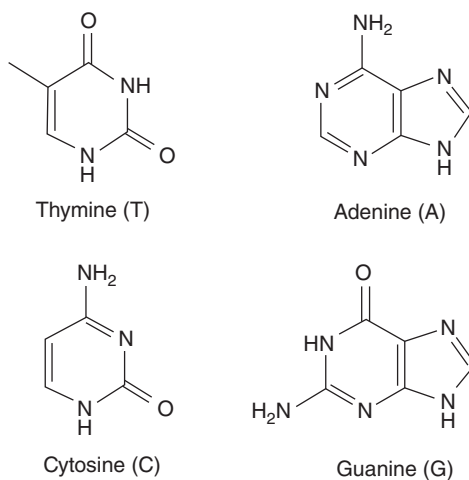
**Figure 1.18** Hydrogen bonding in hierarchical structures of cellulose fibers.

bonds are consolidated within a single structure. For example, cellulose is an example of a molecule where hydrogen bonding can occur both within and between molecules (Figure 1.18). Cellulose is one of the most abundant naturally occurring organic substances, serves as the main structural material of plants, and is the main component of materials such as wood, cotton, and hemp. Cellulose is a polymer – a chain-like molecule composed of many structural repeat units that are covalently bonded together – composed of repeating units of *d*-glucose:

Cellulose molecules readily align themselves in a side-by-side fashion to form fibrils. This is due to hydrogen bonding between the hydroxyl groups ( $-\text{OH}$ ) on each glucose residue. Cellulose fibrils and fibers are extremely strong due to the cooperative nature of these multiple hydrogen bonds. While one hydrogen bond may not provide significant stabilization, there are typically hundreds of hydrogen bonds holding together two cellulose chains, resulting in high strength and low water solubility of the resulting fibril.

Hydrogen bonding is one of the main intermolecular forces that controls DNA hybridization, where single-stranded DNA bonds or *hybridizes* with complementary nucleotide molecules to form double-stranded DNA. As shown in Figure 1.19, DNA strands contain four molecular bases: guanine (G), cytosine (C), adenine (A), and thymine (T).

**Figure 1.19** The four molecular bases of DNA.





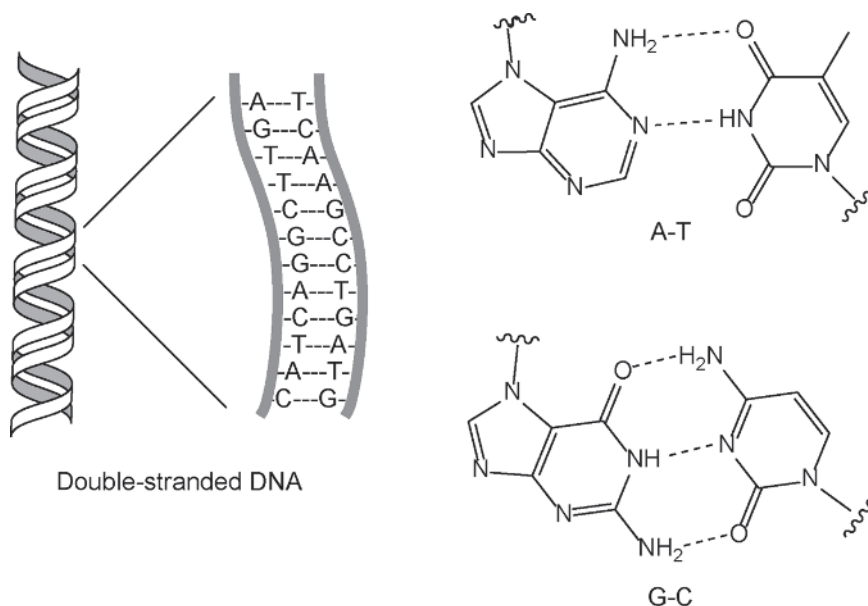


**Figure 1.20** Hydrogen-bonded Watson-Crick base pairs (right) form the hybridized double-stranded DNA structure (left).

Each of these bases undergoes complementary base-pairing through hydrogen bonding: G-C and A-T, also known as Watson-Crick base pairs (Figure 1.20).

G-C base pairs are bound by three hydrogen bonds, while A-T base pairs are bound by only two hydrogen bonds. Base-pairing in DNA hybridization is highly specific due to the geometry of each base: bonding outside of the Watson-Crick base pairs results in a mismatch between hydrogen donors and acceptors, too much steric overlap, or intermolecular distances that are too large to support adequate hydrogen bonding.

### Worked Example 1.8

**Question:** A typical cellulose chain from wood pulp has a length of  $\sim 1000$  glucose units. Estimate the binding strength between two neighboring cellulose chains of this length based on hydrogen bonding interactions alone.

**Answer:** Let us estimate that each glucose unit in a chain of cellulose contributes one hydrogen bond through a hydroxyl group to its neighbor. The binding strength of the  $\text{HO}\cdots\text{H}$  hydrogen bond is  $21 \text{ kJ/mol}$ . The total binding energy can be estimated as:

$$\begin{aligned}
 E &= (1000 \text{ glucose units}) \times \left(1 \frac{\text{bond}}{\text{unit}}\right) \times \left(21 \frac{\text{kJ}}{\text{mol}}\right) \\
 &= 21 \times 10^3 \frac{\text{kJ}}{\text{mol}} \\
 &= 35 \times 10^{-21} \text{ kJ per chain}
 \end{aligned}$$

This is a significant binding strength when compared to the bond energies for strong covalent bonds, such as a single C—C bond ( $\sim 380 \text{ kJ/mol}$ ) or a triple C—C bond ( $\sim 830 \text{ kJ/mol}$ ).

**Worked Example 1.9**

**Question:** Calculate the binding strength of the G-C and A-T base pairs based on hydrogen bonding. Estimate the energy cost to melt – aka “dehybridize” – a double-stranded DNA molecule with 100 bp.

**Answer:** Let us first calculate the binding strength of the base pairs. For the A-T base pair:

$$\begin{aligned} E_{AT} &= E(\text{NH} - \text{O bond}) + E(\text{NH} - \text{N bond}) \\ &= 8 \frac{\text{kJ}}{\text{mol}} + 13 \frac{\text{kJ}}{\text{mol}} = 21 \frac{\text{kJ}}{\text{mol}} \end{aligned}$$

For the G-C base pair:

$$E_{GC} = 2(\text{NH} - \text{O bond}) + (\text{NH} - \text{N bond}) = 29 \frac{\text{kJ}}{\text{mol}}$$

In comparison, the experimental values for the hydrogen bond energies of the base pairs are  $E_{AT} = 13 \text{ kJ/mol}$  and  $E_{GC} = 19 \text{ kJ/mol}$ , indicating that our calculated values overestimate base-pair binding energies.

**1.4 van der Waals Forces**

As shown in Table 1.1, vdW forces – sometimes referred to generally as *dispersion forces* – are characterized by interaction potentials that decay with a scaling law of  $\propto 1/r^6$ . vdW forces are composed of three different types of interactions: Keesom, Debye, and London forces. Since each of these separate interactions possess the same distance dependence, the total vdW interaction potential is the sum of the interaction potentials for these three different contributions:

$$V(r) = \frac{C_w}{r^6} = \frac{C_p}{r^6} + \frac{C_i}{r^6} + \frac{C_d}{r^6} \quad (1.16)$$

where  $C_p$  is the constant for the Keesom force,  $C_i$  is the constant for the Debye force,  $C_d$  is the constant for the London force, and  $C_w$  is a constant that encompasses all three terms. Each of these forces is presented below, along with the potential energy equation used to calculate the corresponding vdW energy of interaction for atoms and small molecules:

**Keesom force.** This force is generated through the interaction of two molecules that each possess permanent dipoles with moments  $\mu_A$  and  $\mu_B$ :

The Keesom force is applicable for dipole–dipole interactions that are not strong enough to cause alignment of the dipoles, unlike the examples in Section 1.4. This can occur for relatively weak dipole moments and dipoles with large separation distances. Instead of a static interaction with fixed dipole orientations, the Keesom force accounts for the net attractive force that occurs between two freely rotating dipoles (Figure 1.21). The potential energy for Keesom interactions,  $V_p$ , is expressed as a function of separation distance,  $r$ :

$$V_p = \frac{C_p}{r^6} = \frac{-\mu_A^2 \mu_B^2}{3(4\pi\epsilon_0)^2 k_B T r^6} \quad (1.17)$$

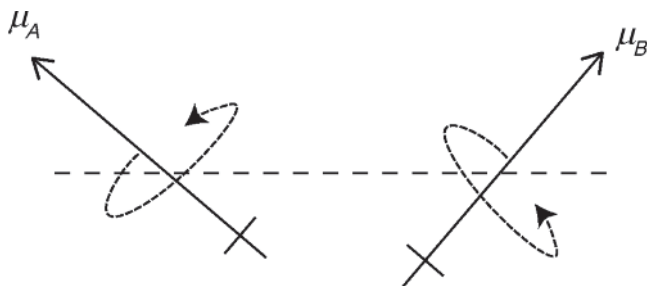


**Figure 1.21** Freely rotating dipole–dipole interaction.

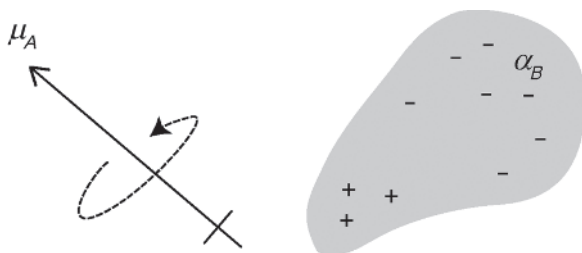


**Figure 1.22** Induced dipole interaction.

where  $C_p$  is a constant and  $T$  is temperature. This contribution averages the energy associated with dipole–dipole interactions over all angular orientations. This interaction is attractive and temperature dependent, since orientation distribution is weighted toward orientations that have lower energies.

**Debye force.** This force is generated through an induced dipole interaction (Figure 1.22), typically between a polar molecule and a nonpolar molecule. The permanent dipole generates a polarizing electric field that induces a dipole moment in a neighboring molecule:

The strength of the induced dipole,  $\mu_{ind}$ , is dependent on the electric polarizability,  $\alpha$ , of the nonpolar molecule, where:

$$\mu_{ind} = \alpha E \quad (1.18)$$

where  $E$  is the electric field generated by the polar molecule. *Polarizability* is a measure of how strongly the negatively charged electron cloud of an atom (or molecule) is displaced relative to its positively charged nucleus in the presence of an applied electric field,  $E$ . It should be noted that  $\alpha$  is often expressed as a volume polarizability in SI units of ( $\text{m}^3$ ), where:

$$\alpha \text{ (m}^3\text{)} = \alpha \text{ (F} \cdot \text{m}^2\text{)} / 4\pi\epsilon_0 \text{ (F/m)} \quad (1.19)$$

For two different molecules each possessing a permanent dipole moment of  $\mu_1$  and  $\mu_2$ , and polarizabilities of  $\alpha_1$  and  $\alpha_2$ , the net potential energy is given as:

$$V_i = \frac{C_i}{r^6} = -\frac{\mu_A^2 \alpha_B + \mu_B^2 \alpha_A}{(4\pi\epsilon_0)^2 r^6} \quad (1.20)$$

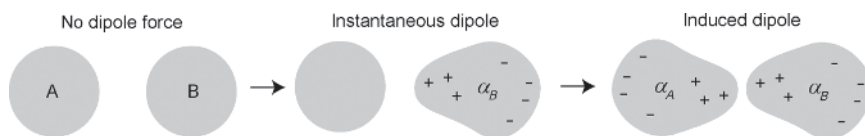


**Figure 1.23** Origin of an instantaneous dipole–dipole interaction.

The above expression provides the energy for the dipole-induced dipole interactions that is averaged overall all angles, since Debye forces are usually too weak to orient molecules.

**London force.** The London or *dispersion* force is generated by transient dipole interactions and is quantum–mechanical in origin. These forces are generated by instantaneous, fluctuating dipole moments generated by the relative positions of electrons and atomic nuclei (Figure 1.23).

The expression for the potential energy of this polarization force is given by the *London equation* for two dissimilar atoms:

$$V_d = \frac{C_d}{r^6} = -\frac{3\alpha_1\alpha_2}{2(4\pi\epsilon_0)^2r^6} \frac{I_1I_2}{(I_1 + I_2)} \quad (1.21)$$

where  $\alpha_1$  and  $\alpha_2$  are the polarizabilities and  $I_1$  and  $I_2$  are ionization energies. Unlike Keesom and Debye forces, dispersion forces are always present and are often the dominant contribution to the total vdW interaction potential (with the exception of highly polar molecules).

### Worked Example 1.10

**Question:** Calculate the vdW binding energy for two Ne atoms separated by a distance of 0.31 nm in vacuum. For Ne, the ionization energy is  $I = 2080$  kJ/mol and the static polarizability is  $\alpha = 0.392 \text{ \AA}^3$ .

**Answer:** Because we are dealing with vdW forces between two atoms, we do not have to consider a dipole force contribution and the binding energy will be dominated by the London equation. Thus, we can plug in these values into the London equation which, for two identical atoms, simplifies to:

$$\begin{aligned} V_d &= -\frac{3I\alpha^2}{4(4\pi\epsilon_0)^2r^6} \\ &= -\frac{3\left(2080 \frac{\text{kJ}}{\text{mol}}\right)(0.392 \text{ \AA}^3)^2}{4(3.1 \text{ \AA})^6} \\ &= -270 \frac{\text{J}}{\text{mol}} \end{aligned}$$

For neutral and nonpolar molecules, vdW forces are always attractive and can serve as a major driving force for binding. For example, liquified and solidified gases (e.g. Ar and Ne) and many organic solvents rely on vdW forces for cohesion. A vdW solid is composed of atoms or molecules that are held together solely by dispersion forces. Many examples of such solids occur for layered materials whose two-dimensional layers are held together by strong vdW forces, such as graphite,

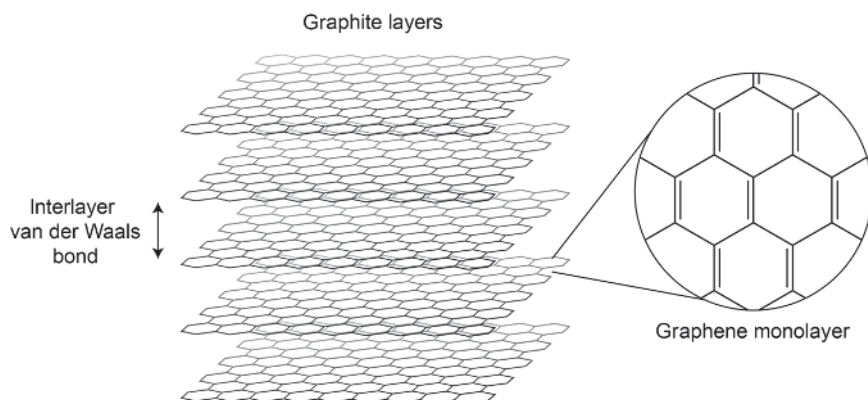


**Figure 1.24** Graphite is composed of atomic layers of graphene that are bound by vdW forces.

MoS<sub>2</sub>, and black phosphorous (Figure 1.24). Because the intermolecular forces that hold vdW solids together are weak compared to covalent or ionic solids, they typically exhibit low melting points.

*vdW forces for particles and surfaces.* How do we calculate the interaction potentials for vdW solids and other nanoscale materials? Unlike electrostatic interactions, vdW forces are not additive. For example, the dispersion interactions between two atoms are affected by other nearby atoms, leading to an interaction potential that can involve three or more atoms. However, we can assume additivity to provide an approximation of the interaction potentials for nano to macroscopic bodies – i.e. objects such as particles, surfaces, and solids that are made up of an infinitesimal number atoms or molecules. For example, let us consider the molecule in Figure 1.25 that is located a distance,  $d$ , away from the surface of a solid slab that is composed of the same molecules with a density,  $\rho$ .

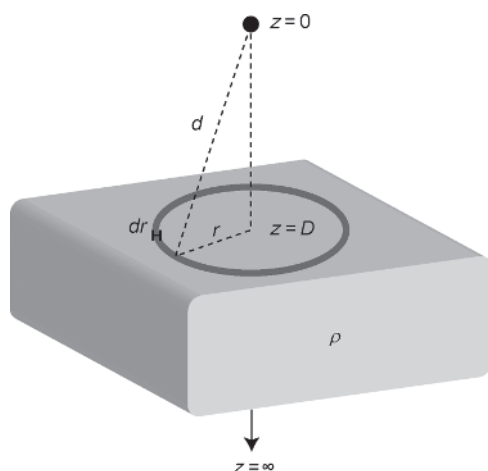


**Figure 1.25** Molecule–surface interaction.

We can define the molecule's location to be  $z = 0$ , and the surface of the slab to be located at  $z = D$ . The total interaction potential energy can be expressed as:

$$V_{mol-surf} = \sum \frac{C_w}{d^6} \quad (1.22)$$

which sums over the energies for the molecule at  $z = 0$  interacting with each molecule in the slab. To sum up the relevant interaction potentials, we can first consider the interaction potential between the molecule and a circular cross-section of the slab with a radius,  $r$ . The total number of molecules in a ring is given by:

$$\text{total \# molecules} = \rho(2\pi r)drdz \quad (1.23)$$

This distance between the molecule and each point in the slab is given by

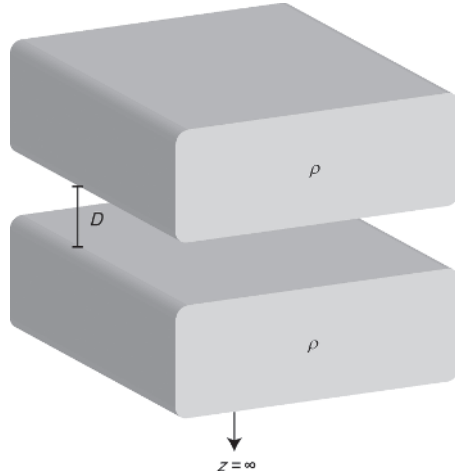
$$d = (r^2 + z^2)^{1/2}$$

such that the total interaction potential can be expressed as the integral:

$$\begin{aligned} V_{mol-surf} &= -2\pi\rho C_w \int_{z=D}^{z=\infty} \int_{r=0}^{r=\infty} \frac{rdrdz}{(r^2 + z^2)^3} \\ &= \pi\rho C_w \int_{z=D}^{z=\infty} \left[ \frac{dz}{2(r^2 + z^2)^2} \right]_{r=0}^{r=\infty} \\ &= \pi\rho C_w \int_{z=D}^{z=\infty} \frac{dz}{2z^4} \\ &= \pi\rho C_w \left[ \frac{1}{6z^3} \right]_{z=D}^{z=\infty} \\ &= \frac{-\pi\rho C_w}{6D^3} \end{aligned} \quad (1.24)$$

We can use the derived expression for  $E_{mol-surf}$  to calculate the interaction potential for two parallel surfaces (Figure 1.26) composed of the same material:

**Figure 1.26** Surface-surface interaction.



by summing over all the molecules on the second surface. Because the interaction energy between two infinite surfaces would itself be infinite, we can instead

calculate the interaction energy,  $V_{surf-surf}$ , per unit area. We then solve for the following expression:

$$\begin{aligned}
 V_{surf-surf} &= -\pi \rho^2 C_w \int_{z=D}^{z=\infty} \frac{dz}{6z^3} \\
 &= \left[ \frac{-\pi \rho^2 C_w}{12z^2} \right]_{z=D}^{z=\infty} \\
 &= \frac{-\pi \rho^2 C_w}{12D^2} \text{ per unit area}
 \end{aligned} \tag{1.25}$$

From our above derivation, we can see the important consequence of summing vdW pair potentials: the interaction energy for larger objects composed of condensed phases decays much more slowly than for individual atoms and molecules. In this case, the interaction energy for two slabs with infinite thickness decays as  $\propto 1/D^2$ , compared to the  $\propto 1/D^6$  scaling law exhibited for two molecules. We typically characterize the strength of an interaction based on this decay length: if a force is *short-range*, it will act on an object at separation distances  $<1$  nm, or near contact. On the other hand, a *long-range* force can act on an object at considerable distances  $>1$  nm. Thus, we can readily see how additive vdW forces can be sufficiently long-range when describing the interactions between nanomaterials.

### Worked Example 1.11

**Question:** Derive an expression for the total vdW interaction energy between two parallel molecular chains (e.g. two linear polymers) that possess a linear density,  $\sigma$ , chain length,  $L$ , and are separated by a short distance,  $D$  (Figure 1.27).

**Answer:** Since two infinitely long chains will possess an infinite interaction energy, we must solve for this expression in terms of chain length,  $L$ . To start, we first sum over all of the interaction between one molecule in chain A with all of the molecules in chain B. We can define the  $x$ -axis along the length of chain B and the  $z$ -axis orthogonal to the two chains (Figure 1.27).

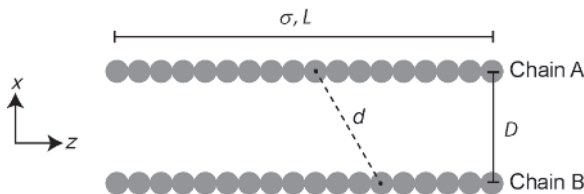


**Figure 1.27** Interaction between two long chains (A and B) with separation distance,  $D$ .

The distance,  $r$ , between the molecule in chain A with those in chain B is given by:

$$d = (x^2 + z^2)^{1/2}$$

and the total number of molecules in chain B with a segment of length  $dx$  is given by:

$$\text{total \# molecules} = \frac{dx}{\sigma}$$

Thus, integrating each molecule–molecule pair potential over the entire length of chain B gives the integral:

$$\begin{aligned} V_{\text{mol-chain}} &= \int_{x=-L/2}^{x=L/2} \frac{-C_w dx}{\sigma d^6} \\ &= \frac{-2C_w}{\sigma} \int_{x=0}^{x=L/2} \frac{dx}{(x^2 + D^2)^3} \end{aligned}$$

Solving for this integral requires some extensive trigonometric substitution (a computer will help here!), but we end up with final expression:

$$V_{\text{mol-chain}} = \frac{-2C_w}{\sigma} \left[ \frac{5D^3x + 3(x^2 + D^2)^2 \tan^{-1}\left(\frac{x}{D}\right) + 3Dx^3}{8D^5 (x^2 + D^2)^2} \right]_{x=0}^{x=L/2}$$

We can approximate this expression for the typical polymer case where  $L \gg D$  to get:

$$\begin{aligned} V_{\text{mol-chain}} &= \frac{-2C_w}{\sigma} \left[ \frac{5}{D^2 L^3} + \frac{3 \tan^{-1}\left(\frac{L}{2D}\right)}{8D^5} + \frac{3}{D^4 L} \right] \\ &= \frac{-C_w}{\sigma} \frac{3\pi}{8D^5} \end{aligned} \quad (1.26)$$

To obtain the interaction energy between the two chains, we then integrate the pair potentials for each molecule along the length of chain A:

$$\begin{aligned} V_{\text{chain-chain}} &= \frac{2}{\sigma} \int_{x=0}^{x=L/2} \frac{-C_w}{\sigma} \frac{3\pi}{8D^5} dx \\ &= \frac{-3\pi C_w}{8\sigma^2} \frac{L}{D^5} \end{aligned} \quad (1.27)$$

The constants in the expression for  $V_{\text{surf-surf}}$  can be more generally expressed as:

$$A = -\pi \rho_A \rho_B C_w \quad (1.28)$$

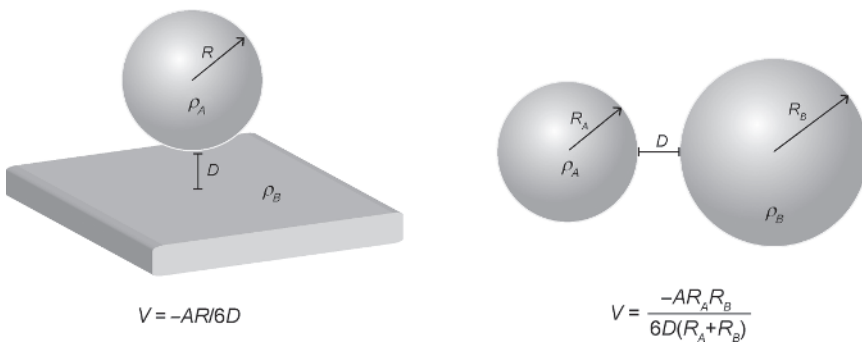
for two interacting bodies with densities  $\rho_A$  and  $\rho_B$ , respectively.  $A$  is known as the *Hamaker constant*, named after the scientist who derived the theory describing vdW forces between macroscopic objects. The Hamaker constant is characteristic for an interacting pair of particles within a given medium. In vacuum, the Hamaker constant for most molecules and materials varies between  $10^{-20}$  and  $10^{-19}$  J, with hydrocarbons at the low end of these values ( $0.01\text{--}5 \times 10^{-20}$  J) and metals at the high end ( $15\text{--}45 \times 10^{-20}$  J). Table 1.2 lists some general values of the Hamaker constants for some common materials in vacuum. The Hamaker constant is convenient when describing the vdW interaction potentials between objects with different shapes, for which expressions can be derived by additive pair potentials. For example, using a similar approach to the previous worked example, the following expression can be derived for a sphere approaching a surface composed of the same material:

$$V(D)_{\text{sphere-surf}} = \frac{-AR}{6D} \quad (1.29)$$



**Table 1.2** Hamaker constants used to calculate the energies between interacting bodies composed of the material listed, in vacuum.

Material	Hamaker constant ( $10^{-20}$ J)
Au	45.5
Ag	40.0
Cu	28.4
Si	25.6
Ge	30.0
Al <sub>2</sub> O <sub>3</sub>	15.5
TiO <sub>2</sub> (anatase)	19.7
TiO <sub>2</sub> (rutile)	31.1
CdS	15.3
SiO <sub>2</sub>	16.4
Graphite	47
Diamond	28.4
Water	4.4
Decane	5.0
Polystyrene	6.2
Polyvinyl alcohol	8.8

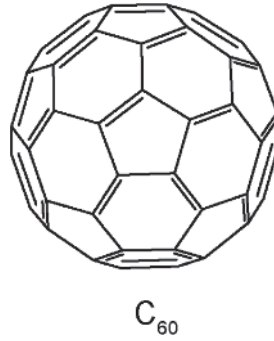


**Figure 1.28** Sphere-surface and sphere-sphere interaction potentials.

where  $R$  is the radius of the sphere and  $D$  is the surface-to-surface separation distance. Similarly, we can derive an expression for two approaching spheres composed of the same material:

$$V(D)_{\text{sphere-sphere}} = \frac{-AR_A R_B}{6D(R_A + R_B)} \quad (1.30)$$

where  $R_A$  and  $R_B$  are the radii of the spheres. Figure 1.28 depicts these two pairwise geometries which are commonly found in nanoscale systems.

**Figure 1.29**  $C_{60}$  molecule.**Worked Example 1.12**

**Question:** Shown in Figure 1.29,  $C_{60}$  condenses into solid with a density of  $1.65 \text{ g/cm}^3$  at room temperature. Molecular  $C_{60}$  possesses a polarizability of  $76.5 \times 10^{-30} \text{ m}^3$ , a dipole moment of  $\mu = 0 \text{ D}$ , an ionization energy of  $IE = 7.5 \text{ eV}$ , and a diameter of  $0.7 \text{ nm}$ . Using these molecular parameters, estimate the Hamaker constant for condensed  $C_{60}$ .

**Answer:** The equation for the Hamaker constant can be simplified to:

$$A = -\pi \rho_A \rho_B C_w = -\pi (\rho_{C_{60}})^2 C_d$$

since molecular  $C_{60}$  is nonpolar and only London dispersion forces contribute to  $C_w$ . First, we transform the density of condensed  $C_{60}$  into a number density:

$$\begin{aligned} \rho_{C_{60}} &= \frac{\text{number of molecules}}{\text{volume}} \\ &= 1.65 \text{ g/cm}^3 \times \frac{6.02 \times 10^{23} \text{ molecules}}{(12.01 \text{ g})(60)} \times \frac{1 \text{ cm}^3}{10^{-6} \text{ m}^3} \\ &= 1.38 \times 10^{27} \text{ m}^{-3} \end{aligned}$$

We can then use the London equation to calculate  $C_d$  for two  $C_{60}$  molecules:

$$\begin{aligned} C_d &= -\frac{3\alpha^2 I}{4(4\pi\epsilon_0)^2} \\ &= -\frac{3}{4} (76.5 \times 10^{-30} \text{ m}^3)^2 (1.2 \times 10^{-18} \text{ J}) \\ &= -5.3 \times 10^{-75} \text{ J} \cdot \text{m}^6 \end{aligned}$$

Putting this altogether, we can calculate  $A$  as:

$$\begin{aligned} A &= -\pi \rho_A \rho_B C_w \\ &= -\pi (1.38 \times 10^{27} \text{ m}^{-3})^2 (-5.3 \times 10^{-75} \text{ J} \cdot \text{m}^6) \\ &= 3.2 \times 10^{-20} \text{ J} \end{aligned}$$

This value comes reasonably close to the value of the Hamaker constant ( $7.5 \times 10^{-20} \text{ J}$ ) derived from experimental measurements of  $C_{60}$  interactions in water.

**Worked Example 1.13**

**Question:** Graphite is a layered solid that is held together only through vdW interactions. The Hamaker constant for graphite interacting across air is  $A = 47 \times 10^{-20}$  J. Calculate the binding energy between two slabs of graphite separated by 1 nm.

**Answer:** Using Eq. 1.31, we calculate:

$$\begin{aligned} V_{\text{surf-surf}} &= \frac{-A}{12D^2} \text{ per unit area} \\ &= \frac{-47 \times 10^{-20} \text{ J}}{12(1 \times 10^{-9} \text{ m})^2} \\ &= -39 \times 10^{-3} \text{ J/m}^2 \end{aligned}$$

## 1.5 Hydrophobic Forces

Hydrophobic forces refer to the attraction between nonpolar molecules, particles, and surfaces in the presence of water. These hydrophobic (a word derived from the ancient Greek words for “water-fearing”) bodies experience a strong mutual attraction that is responsible for a wide range of phenomena, including the formation of surfactant micelles, cell membranes, and protein folding. This strong attraction often results in spontaneous ordering or *assembly* of hydrophobic molecules, as depicted for surfactants in Figure 1.30, such that water is expelled into the bulk.

However, unlike the intermolecular forces discussed in previous sections, there is no universal force law to describe the multitude of experimental observations that are attributed to hydrophobic forces. Hydrophobic forces have been observed to operate over both long-range (20–300 nm) and short-range (<20 nm). The derivation of a force law is also complicated by the knowledge that water molecules hydrate small versus large hydrophobic solutes in very different ways.

At the molecular scale, hydrophobic forces are attributed to the restructuring of  $\text{H}_2\text{O}$  molecules around hydrophobic solutes. In the bulk liquid state,  $\text{H}_2\text{O}$  has a strong tendency to form hydrogen bonds with four other neighboring  $\text{H}_2\text{O}$  molecules, giving rise to tetrahedral coordination (Figure 1.31). However, this coordination is *labile* since the lifetimes of these hydrogen bonds are short ( $<10^{-11}$  s), allowing the intermolecular  $\text{H}_2\text{O}$  bonds to associate and dissociate rapidly. Hydrogen bond length in bulk liquid water also depends strongly on temperature and pressure. (It should be noted that there is still debate over what constitutes a “broken” hydrogen bond in water, as defined by either a critical bond length and/or bond angle.)

When a hydrophobic solute is introduced into liquid water, attractive forces between the solutes arise primarily due to a change in *entropy*. Let’s consider a simple hydrocarbon – an organic compound composed entirely of H and C atoms – such as the hexane molecule,  $\text{C}_6\text{H}_{14}$ , shown in Figure 1.32. To solvate hexane,  $\text{H}_2\text{O}$  molecules must break their tetrahedral coordination and reorganize to accommodate  $\text{C}_6\text{H}_{14}$  molecules. In effect, this forms a cavity in bulk water due to  $\text{H}_2\text{O}$ – $\text{H}_2\text{O}$  hydrogen bond-breaking:

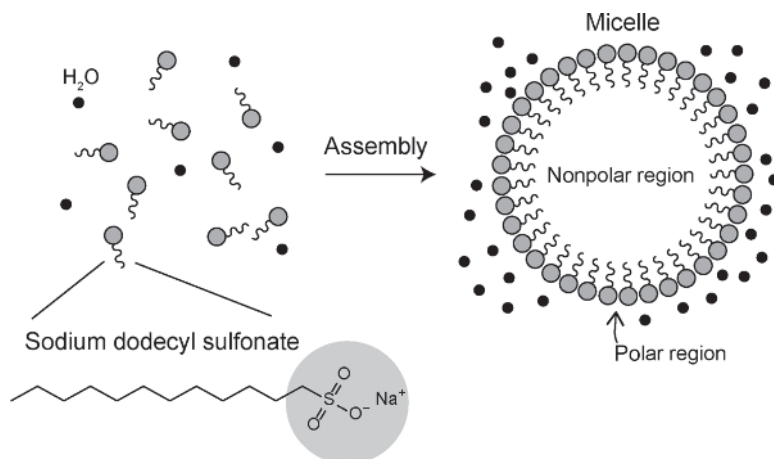
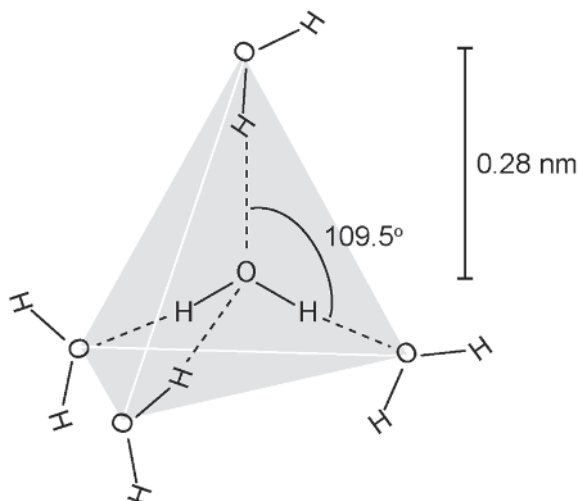


**Figure 1.30** Surfactants such as sodium dodecyl sulfonate are amphiphilic molecules that can spontaneously order into spherical structures called micelles.

**Figure 1.31** The tetrahedral structure of hydrogen-bonded water molecules in ice.



The  $\text{H}_2\text{O}$  molecules directly around the solute can compensate for this change in enthalpy ( $\Delta H$ ) by forming extra hydrogen bonds with its nearest  $\text{H}_2\text{O}$  neighbors to generate a cage-like  $\text{H}_2\text{O}$  structure. In our example,  $\Delta H = 0 \text{ kJ/mol}$  for transferring a  $\text{C}_6\text{H}_{14}$  from a nonpolar solvent to water; in other words, there is no enthalpic cost for mixing hexane and water. However, the entropic cost for forming the ordered  $\text{H}_2\text{O}$  cage is significant ( $\Delta S = 28 \text{ kJ/mol}$ ). The driving force for  $\text{C}_6\text{H}_{14}$  to self-segregate is the reduction in the number of  $\text{H}_2\text{O}$  molecules participating in these cage structures, which are entropically unfavored.

These short-range hydrophobic interactions are typically considered the main driving force for the formation of a variety of self-assembled structures, such as

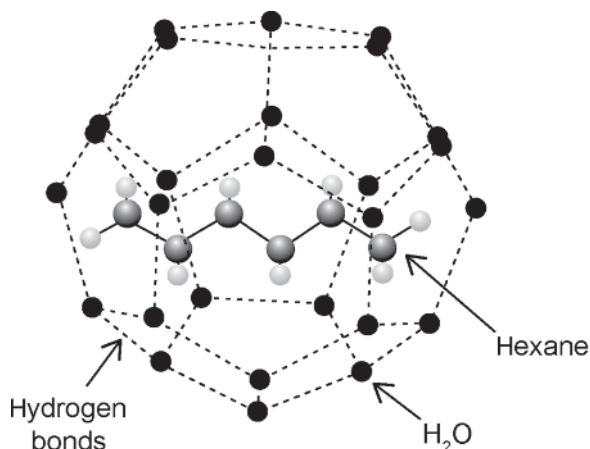


**Figure 1.32** Water molecules form ordered, cage-like structures around nonpolar molecules like hexane.

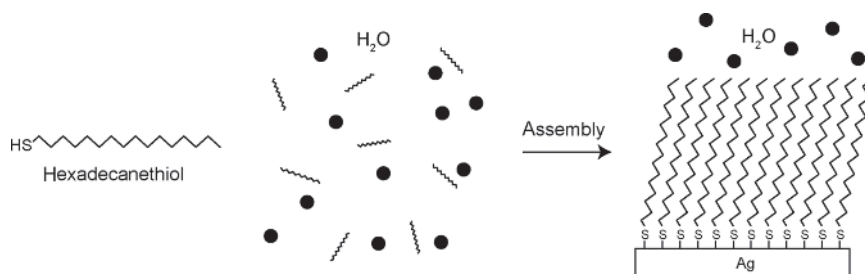


**Figure 1.33** Self-assembled monolayers (SAMs) are formed by the spontaneous organization of alkanethiols in the presence of a metal surface, such as Ag or Au.

*self-assembled monolayers* (often abbreviated as SAMs) and *liposomes*. SAMs consist of molecules that organize into packed layers that are only a single-molecule thick (Figure 1.33). They are commonly used to passivate a variety of solid surfaces and nanoscale materials, such as metal nanoparticles, since the molecular monolayer forms a physical barrier against further chemical interactions or reactions. They typically comprise molecules that contain a hydrophobic component and a head group – a functional group located at the end of the molecule. The head group serves as a molecular anchor, forming a coordination or covalent bond to the solid surface. For example, alkanethiols are commonly used to form SAMs on metal Au and Ag surfaces. The thiol ( $-\text{SH}$ ) head group serves as a *ligand* that deprotonates and binds to metal atoms to form a strong  $\text{Au}-\text{S}$  or  $\text{Ag}-\text{S}$  bond. However, the hydrophobic forces derived from the long alkane chain are the driving force for molecular organization into a dense hydrophobic layer.

Liposomes are an example of a self-assembled nanostructure that results largely from hydrophobic interactions (Figure 1.34). Liposomes are typically formed from phospholipids, the same molecules that comprise cell membranes:

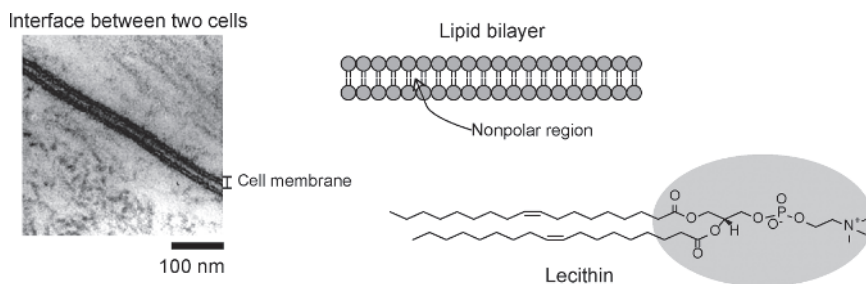


**Figure 1.34** A transmission electron microscope image of the region where two cells touch (left). The dark regions show the electron-dense portion (circled, right) of the phospholipid comprising the cell membrane. Lecithin (right) is a representative phospholipid and a chief component of cell membranes.

While a cell membrane is considered a two-dimensional assembly of phospholipids, a liposome is a three-dimensional artificial vesicle that consists of fluid enclosed within a lipid bilayer (Figure 1.35). Unlike a micelle, a liposome possesses both hydrophilic interior and exterior surfaces. They are extensively used as encapsulants in the cosmetic and pharmaceutical industries because they can be employed to deliver both hydrophobic and hydrophilic molecules and because the phospholipid bilayer can be embedded with biological targeting groups. The liposome, similar to a SAM, forms a physical barrier around its contents that allow molecular payloads to be protected from oxidation and degradation processes.

While short-range hydrophobic interactions are relatively well understood, the fundamental mechanism behind long-range hydrophobic forces is still an active area of research. Long-range forces can be categorized as the attractive force that develops between hydrophobic surfaces, leading to phenomena such as the self-assembly of hydrophobic nanoparticles, with examples shown in Figure 1.36.

In some experimental cases, the observed attractions are not considered purely hydrophobic in nature and result from a combination of electrostatic and

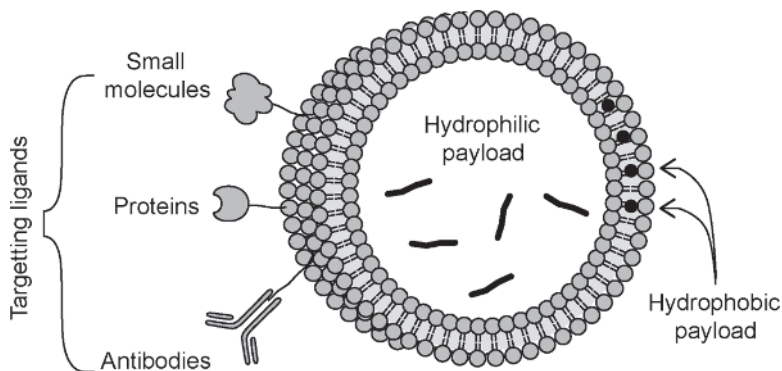


**Figure 1.35** Liposomes are spherical structures composed of lipid bilayers. They can be used to encapsulate payloads in different regions and can be chemically modified to target specific biological entities.

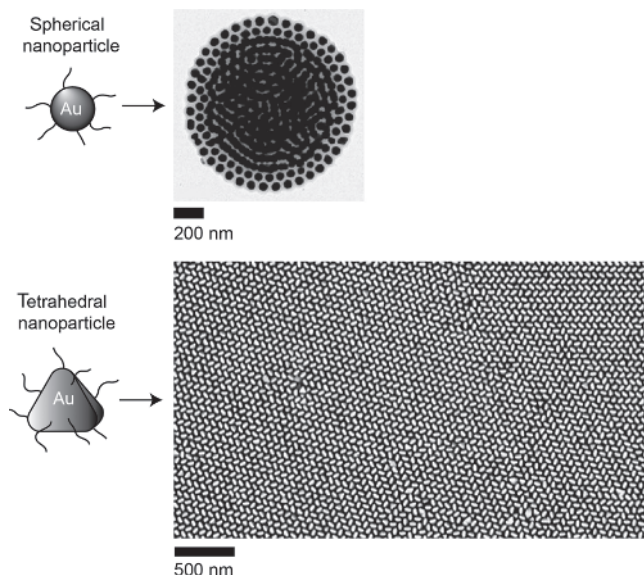


**Figure 1.36** Au nanoparticles modified with hydrophobic ligands can undergo spontaneous self-organization into superstructure due to hydrophobic forces. Top: Spherical nanoparticle form nanoparticle micelles. Source: Reproduced from ACS Nano 2012, 6, 12, 11059–11065. Bottom: Hydrophobic tetrahedral nanocrystals form a herringbone superstructure. Source: Reproduced from J. Am. Chem. Soc. 2022, 144, 30, 13538–13546.

hydrophobic interactions that contribute to a long interaction distance. In other cases, it is proposed that  $\text{H}_2\text{O}$  molecules near the hydrophobic solute cause a local change in the Hamaker constant, enhancing the vdW interaction between hydrophobic surfaces by a significant amount. In the coming years, it is likely that advances in multiscale modeling – theoretical models that span multiple time and length scales – will pave the way in understanding how these various molecular-level effects contribute to long-range hydrophobic interactions and their corresponding phenomena.

## 1.6 Steric Forces

Steric repulsion results from the overlap in electron clouds for two approaching atoms or molecules at very short (interatomic,  $<1$  nm) distances. This force can be both quantum–mechanical and electrostatic in nature. The quantum–mechanical component stems from the *Pauli exclusion principle*, which dictates that no two electrons share the same quantum state. The electrostatic component arises from *Born repulsion* between similarly charged electrons or from the repulsive interaction between two positively charged nuclei. As such, there is no universal force law that describes how steric interactions change with respect to distance. However, several empirical functions have been developed that adequately describe the behavior of this short-range repulsive potential.

One of the most well-known empirical functions is the *power-law potential*, of the form:

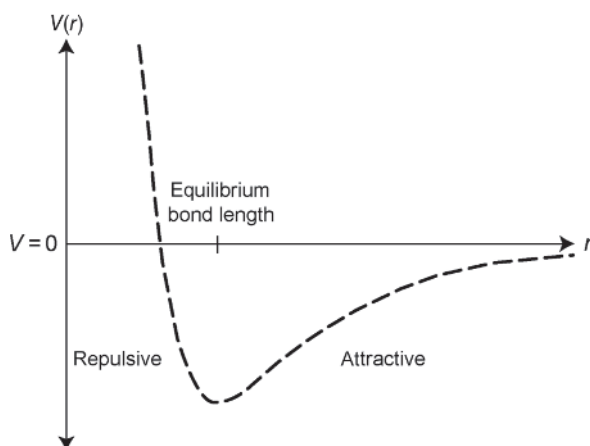
$$V = \left(\frac{\sigma}{r}\right)^n \quad (1.31)$$

where  $n$  is an integer usually between 9 and 16. The power-law potential is the form of the repulsive potential used in the Lennard-Jones or “6–12” potential:

$$V = \frac{A}{r^{12}} - \frac{B}{r^6} \quad (1.32)$$

where  $A$  and  $B$  are integers, and  $r$  is the intermolecular distance. The Lennard-Jones potential combines the attractive pair potential resulting from vdW interactions with a repulsive pair potential describing steric interactions. The total potential plotted in Figure 1.37 shows the appearance of a potential well:

**Figure 1.37** The Lennard-Jones potential.



where energy is minimized at a separation distance that is typically associated with equilibrium bond length. The equilibrium bond length obtained for the Lennard-Jones potential can be used to determine the *van der Waals radius* of a molecule, which is defined as the radius of the imaginary hard sphere surrounding the molecule.

### Worked Example 1.14

**Question:**  $C_{60}$  is a nonpolar molecule with no net charge, whose intermolecular interactions can be described by the Lennard-Jones potential (with constants  $A = 34.8 \times 103 \text{ eV } \text{\AA}^{12}$  and  $B = 20 \text{ eV } \text{\AA}^6$ ). Calculate the equilibrium bond length and binding energy for two  $C_{60}$  molecules in vacuum.

**Answer:** The pair potential between two  $C_{60}$  molecules is described by

$$V(r) = \frac{A}{r^{12}} - \frac{B}{r^6}$$

The bond length can be found by calculating the separation distance between the molecules at equilibrium, when the net force between two  $C_{60}$  molecules is zero:



$$F = -\frac{dV(r)}{dr} = 0$$

$$= \frac{d}{dr} \left( \frac{A}{r^{12}} - \frac{B}{r^6} \right) = \frac{-6A}{r^{11}} + \frac{6B}{r^5}$$

Solving for  $r$  and substituting the Lennard-Jones constants, we get:

$$r = \left( \frac{2A}{B} \right)^{1/6} = \left( \frac{2 \cdot 34.8 \times 10^3 \text{ eV} \cdot \text{\AA}^{12}}{20 \text{ eV} \cdot \text{\AA}^6} \right)^{1/6} = 3.89 \text{ \AA}$$

To calculate the binding energy, we plug this value back into our equation for  $V(r)$ :

$$V(3.89 \text{ \AA}) = \frac{34.8 \times 10^3 \text{ eV} \cdot \text{\AA}^{12}}{(3.89 \text{ \AA})^{12}} - \frac{20 \text{ eV} \cdot \text{\AA}^6}{(3.89 \text{ \AA})^6}$$

$$= -2.87 \text{ meV}$$

$$= -2.77 \text{ kJ/mol}$$

Steric forces determine how close atoms and molecules can be situated from one another. This can have a profound effect on the chemical reactivity of molecules, nanomaterials, and surfaces. For example, steric *hindrance* occurs when chemical reactions are slowed due to the presence of bulky side groups or substituents of molecules. In chemical synthesis, steric hindrance can be engineered to block unwanted side reactions. In a similar manner, steric repulsion also has important

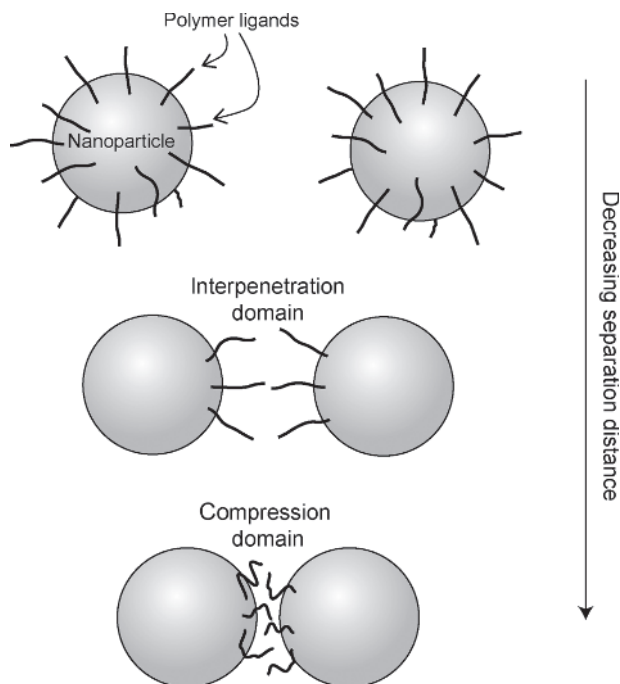


**Figure 1.38** Polymer-grafted nanoparticle experience steric repulsion as they approach each other.

consequence for nanomaterials that are passivated by bulky molecules, such as polymers or SAMs. Molecular passivation layers control access to the surface, and thus contribute greatly to the thermodynamic, chemical, and physical properties of a nanomaterial.

Let us consider two nanoparticles that are grafted (i.e. chemically bound or anchored) with several polymer chains, as drawn in Figure 1.38. As the nanoparticles approach each other, they experience an increasing repulsive force due to steric overlap between the polymer chains that are trapped between the particles. This is usually described by two regions: (i) the interpenetration domain and (ii) the compression domain. The interpenetration domain is typically characterized by polymer–solvent interactions and occurs at interparticle distances of 1–2 polymer chain lengths. The compression domain occurs at shorter interparticle distances; in this regime, steric overlap causes the polymer grafts to adopt “compressed” configurations. This results in a decrease in the free volume – the unfilled void space associated with a molecule – of the polymer chains as the particles approach. This compression is entropically unfavorable and, thus, increases the free energy of the system. As a result, such nanoparticles are considered *entropically stabilized* because the polymer grafts generate this entropic steric repulsion upon close approach. The magnitude of this repulsive force is dependent on both the surface density and the free volume of the polymer grafts.

### Worked Example 1.15

**Question:** Consider a dispersion of polymer-grafted nanoparticles in water that are stabilized mainly due to entropic interactions. How do you expect the aggregation state of these nanoparticles to change upon heating or cooling?

**Answer:** We can consider the overall Gibbs free energy of the nanoparticle system as

$$\Delta G = \Delta H - T\Delta S$$

where an increase or decrease in temperature modifies the entropic contribution in the second term. Heating the system increases the overall entropic contribution, and we would expect the nanoparticles to remain in a stable dispersion. Cooling decreases the overall entropic contribution and would likely destabilize the dispersion toward an aggregated or metastable state.

## 1.7 Particle Stability and Aggregation

Let us revisit our example of nanoparticles dispersed in a liquid medium from Figure 1.1. How do different intermolecular forces contribute to the behavior of such a nanoscale system? We can consider the case where our nanoparticles are subject to both repulsive *and* attractive interactions. The resulting pair potential would be the sum of multiple contributing pairwise potentials. The graphs in

Figure 1.39 show two very different cases that result from the addition of repulsive and attractive potential energy terms with varying magnitudes:

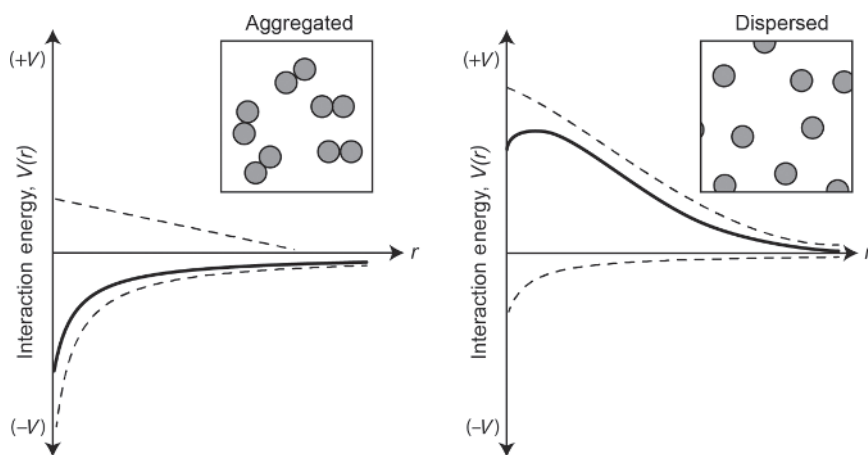


**Figure 1.39** Two examples of pairwise potentials (solid line) that result from summing different repulsive and attractive interactions (dashed lines). A weak repulsive interaction leads to aggregated particles (left), while a weak attractive interaction leads to dispersed particles (right).

As we can see, the overall behavior of the nanoparticle dispersion will depend entirely on the relative strengths of the two forces at play. For the plot on the left, the pair potential exhibits a relatively weak repulsive interaction but a strong attractive interaction. Because the energy minimum occurs at  $r = 0$ , the nanoparticles will likely *aggregate* to form dimers or larger clusters. For the plot on the right, the pair potential exhibits a relatively strong repulsive interaction and only weak attraction. The minimum potential energy is achieved at  $r \rightarrow \infty$ ; hence, the nanoparticles will stay suspended in the medium as a dispersed system.

In some cases, the pairwise potential exhibits multiple potential energy minima, such as the plot shown in Figure 1.40. These nanoparticle systems can exist in *metastable* states. For example, in the plot shown in Figure 1.40, the energy minimum occurs at  $r = 0$ . However, the nanoparticles may stay trapped in a local potential energy minimum by maintaining a separation distance greater than  $r_1$ . For  $r > r_1$ , the potential energy is negative and stability is achieved as  $r \rightarrow \infty$ , even though it does not represent the absolute minimum energy that could be attained. This is often referred to as a metastable dispersion, since aggregation is limited by the energy barrier located at  $r_2$ , depending on its height ( $\Delta V$ ). If  $\Delta V$  is small, the particles will aggregate ( $r \rightarrow 0$ ); if  $\Delta V$  is large, the particles will stay dispersed ( $r \rightarrow \infty$ ).  $\Delta V$  is typically measured in units of thermal energy,  $k_B T$  (where  $k_B T = 4.11 \times 10^{-21}$  J at room temperature) and serves as a gauge for whether aggregation will occur.

Aggregation becomes an increasingly important consideration as particle size decreases. At the nanoscale, attractive vdW forces become competitive with steric

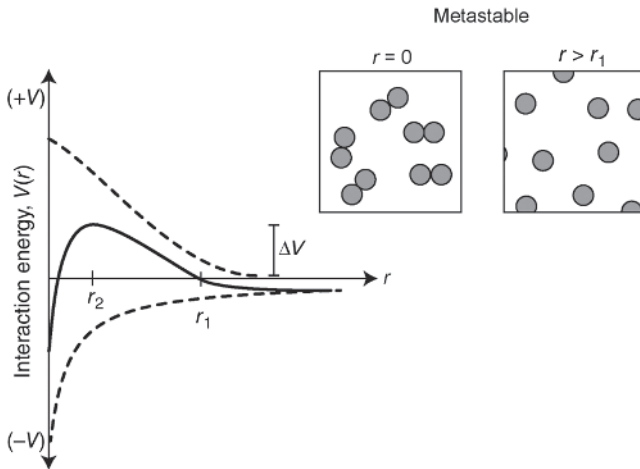


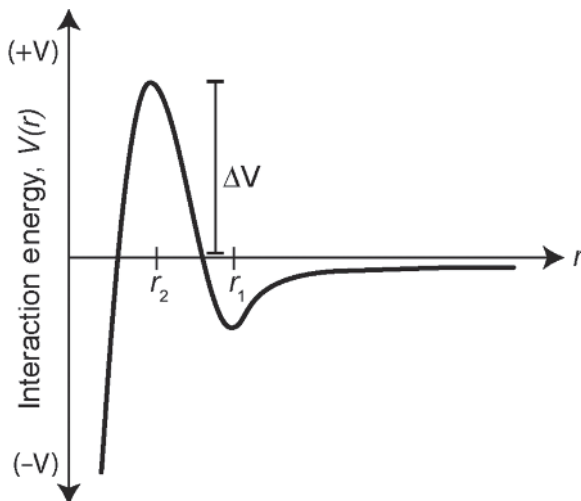
**Figure 1.40** The sum of attractive and repulsive interactions (dashed lines) can lead to a pairwise potential that exhibits metastability.

and electrostatic repulsion, leading to different types of aggregation phenomena. This is not often the case for macroscopic objects (e.g. particles of sand), which require different long-range forces (such as gravity or capillary forces) to generate adhesion.

### Worked Example 1.16

**Question:** Consider a dispersion of nanoparticles that exhibit the pairwise potential below (Figure 1.41). Describe the aggregation behavior of the nanoparticles for the two different cases: (i)  $\Delta V \gg 0$  and for (ii)  $\Delta V \approx 0$ .

**Figure 1.41** Possible pair potential for nanoparticles.



**Answer:** The pairwise potential above is characterized by an energy minimum at  $r_1$ , an energy barrier at  $r_2$ , and a deep energy well as  $r$  approaches 0. For case (i), the nanoparticles would likely come into stable equilibrium to form clusters with an interparticle separation distance of  $r_1$ . The presence of a large energy barrier would cause the nanoparticles to remain kinetically stable at this separation distance. For case (ii), the nanoparticles would likely adhere into structures with a separation distance of  $r_1$  (a metastable state) and then slowly aggregate.

### Worked Example 1.17

**Question:** Two perfectly spherical silica ( $\text{SiO}_2$ ) nanoparticles with a diameter of 30 nm are coated with a negatively charged surface coating and are separated by a distance of 5 nm. For what surface charge density does the repulsive electrostatic potential become equal but opposite to the attractive vdW potential?

**Answer:** First, we can calculate the pairwise potential for the vdW interaction between the two nanoparticles. From Table 1.2, we see that  $A_{\text{SiO}_2} = 16.4 \times 10^{-20} \text{ J}$ . Plugging this into the vdW expression for two interacting spheres, we get:

$$V = \frac{-AR}{12D} = \frac{-(16.4 \times 10^{-20} \text{ J})(15 \times 10^{-9} \text{ m})}{12(5 \times 10^{-9} \text{ m})} = -41 \times 10^{-21} \text{ J}$$

We can then plug this binding energy into the expression for electrostatic potential between two point charges to calculate the total charge,  $Q$ , for each nanoparticle. Recall that in this expression,  $r$  is the center-to-center distance between the particles.

$$V = \frac{Q^2}{4\pi\epsilon\epsilon_0 r} = 41 \times 10^{-21} \text{ J}$$

$$\frac{Q^2}{4\pi \left( 8.85 \times 10^{-12} \frac{\text{C}^2}{\text{J} \cdot \text{m}} \right) (35 \times 10^{-9} \text{ m})} = 41 \times 10^{-21} \text{ J}$$

$$Q = -4.0 \times 10^{-19} \text{ C}$$

We can then plug this total charge into the equation for surface charge density,  $\sigma$ :

$$\sigma = \frac{Q}{A} = \frac{-4.0 \times 10^{-19} \text{ C}}{4\pi(15 \times 10^{-9} \text{ m})^2} = -1.4 \times 10^{-4} \text{ C/m}^2$$

To put this in context, this surface charge density is equivalent to one negative ion per every 1000  $\text{nm}^2$  or equivalently a rough separation distance of 30 nm on the surface of the nanoparticle.

## Further Reading

Berg, J.C. (2010). *An Introduction to Interfaces & Colloids: The Bridge to Nanoscience*. World Scientific.

Hammer, M.U., Anderson, T.H., Chaimovich, A. et al. (2010). The search for the hydrophobic force law. *Faraday Discussions* 146: 299–308.

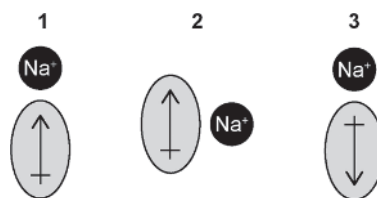
Israelachvili, J.N. (2011). *Intermolecular and Surface Forces*. Academic press.

- Rogers, B., Adams, J., and Pennathur, S. (2014). *Nanotechnology: Understanding Small Systems*. CRC Press.
- Silverstein, T.P. (1998). The real reason why oil and water don't mix. *Journal of Chemical Education* 75 (1): 116.
- Ulman, A. (2013). *An Introduction to Ultrathin Organic Films: From Langmuir-Blodgett to Self-Assembly*. Academic press.

## Problems and Discussion Topics

- 1.1 List the intermolecular forces that you would expect to occur between ethanol ( $\text{C}_2\text{H}_5\text{OH}$ ) and water ( $\text{H}_2\text{O}$ ) molecules, in order of increasing strength.
- 1.2 List the following liquids in order of lowest to highest boiling points and briefly explain the reasoning behind your answer:  $\text{H}_2\text{O}$ ,  $\text{H}_2\text{S}$ ,  $\text{H}_2\text{Se}$ , and  $\text{H}_2\text{Te}$ .
- 1.3 List the following molecules in order of dipole moment, from smallest to largest:  $\text{CO}$ ,  $\text{CO}_2$ ,  $\text{CHCl}_3$ ,  $\text{C}_6\text{H}_6$ , and  $\text{CH}_3\text{OH}$ .
- 1.4  $\text{NH}_3$  has a dipole moment of 1.47 D. Consider the interaction energy between  $\text{Na}^+$  and  $\text{NH}_3$  in an aqueous solution with a separation distance of 0.2 nm ( $\epsilon_{\text{H}_2\text{O}} = 80.10$ ). Calculate the interaction potential for each of the ion-dipole orientations shown below (Figure 1.42) and determine the orientation with the lowest potential energy.

Figure 1.42 Dipole-ion interactions.



- 1.5 If there is a uniformly spaced line of alternating anions and cations with a distance,  $d$ , between the centers of the ions, show that the interaction energy is given by:

$$E = \frac{\epsilon^2}{4\pi\epsilon_0} \frac{Z_A Z_B}{d} 2 \ln 2$$

- 1.6 Plot the interaction potential for a  $\text{Na}^+$  ion and  $\text{Cl}^-$  ion as a function of separation distance in three different solvents:
  - (a) Water ( $\epsilon = 80.2$ )
  - (b) Ethylene glycol ( $\epsilon = 37$ )
  - (c) Chloroform ( $\epsilon = 4.8$ )

- 1.7** Calculate the Debye lengths and compare the screened electric fields,  $V(r)$ , for a nanoparticle dispersed in 10 mM  $\text{CaCl}_2$  versus 10 mM  $\text{MgSO}_4$ .
- 1.8** Calculate the Debye length for phosphate-buffered saline (PBS), which is a commonly used medium to mimic the physiological conditions of the human body. PBS is composed of the following electrolytes: 137 mM  $\text{NaCl}$ , 2.7 mM  $\text{KCl}$ , 10 mM  $\text{Na}_2\text{HPO}_4$ , and 1.8 mM  $\text{KH}_2\text{PO}_4$ . How does Debye screening in PBS impact nanoscale devices designed to go into the human body?
- 1.9** The electric polarizability of a fullerene molecule of  $\text{C}_{60}$  has been measured as  $76.5 \text{ \AA}^3$ . Calculate the induced dipole moment,  $\mu_{\text{ind}}$ , on  $\text{C}_{60}$  in the presence of a  $\text{Na}^+$  ion located at a center-to-center distance of 2 nm away. How do you expect this value of  $\mu_{\text{ind}}$  to compare to a molecule of methane ( $\text{CH}_3$ )? How about a carbon nanotube?
- 1.10** The pairwise potential in Figure 1.43 describes the aggregation behavior of positively charged nanoparticles dispersed in a  $\text{NaCl}$  solution.

Qualitatively plot how you would expect the pairwise potential to change under the following experimental conditions:

- Large increase in  $[\text{NaCl}]$
- Large decrease in  $[\text{NaCl}]$
- Change in electrolyte to  $\text{CaCl}_2$  with equivalent molar concentration.

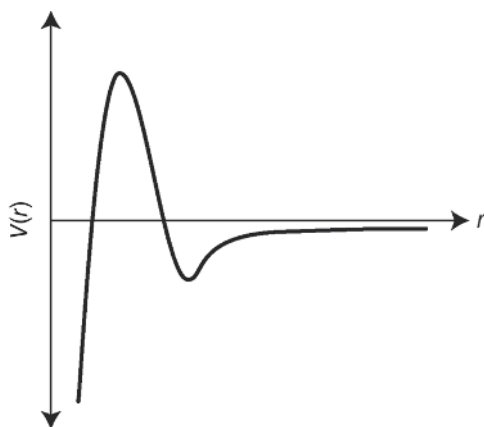


**Figure 1.43** Possible pair potential for charged nanoparticles.

- 1.11** The heat of sublimation for Ne can be used to measure the bond dissociation energy for pure Ne, which is approximately 2 kJ/mol. Explain this discrepancy with the vdW pair potential for two Ne atoms calculated in the worked example.
- 1.12** Spontaneous opening of DNA's double helix structure to form single-stranded DNA is a rare event, but double-stranded DNA can be readily

“melted” to form single-stranded DNA by heating. Using your knowledge of base-pair interactions, formulate a simple expression for calculating the melting temperature of a DNA strand with a given sequence.

- 1.13** Derive the following expression for the induced dipole imparted by a polar molecule with a fixed orientation,  $\vartheta$ , and dipole moment,  $\mu$ , and a nonpolar molecule with polarizability,  $\alpha$ , located at a separation distance of  $r$ :

$$\mu_{ind} = \frac{\mu\alpha\sqrt{(1 + 3\cos^2 \theta)}}{4\pi\epsilon\epsilon_0 r^3}$$

- 1.14** Consider a spherical particle with a radius,  $R$ , and a flat surface made of identical material separated at some distance,  $D$ , and held together only by vdW interactions. The *effective area of interaction* is defined as the area for which two flat surfaces at the same separation distance would have the same interaction force. Calculate the effective area of interaction of the spherical particle.
- 1.15** In a solution of polymer, a poor solvent can turn into a good solvent by increasing the temperature to a critical point called the *theta temperature*. Explain why miscibility is temperature dependent.
- 1.16** The bond strength of an  $H_2$  molecule is 436 kJ/mol. The distance at which the bond breaks ( $V = 0$ ) is 2.93 Å. Using the Lennard-Jones potential:  
 (a) Calculate the equilibrium bond distance for  $H_2$ .  
 (b) Calculate the maximum adhesion force between the two H atoms.
- 1.17** For the Lennard-Jones potential, what is the predicted equilibrium separation distance for the minimum energy of interaction? What is the predicted separation distance when the adhesive force,  $F$  is maximum?
- 1.18** The diameter of  $C_{60}$  is 0.71 nm and the Lennard-Jones potential constants are  $A = 34.8 \times 10^3 \text{ eV } \text{\AA}^{12}$  and  $B = 20 \text{ eV } \text{\AA}^6$ .  
 (a) What are the intermolecular forces that drive fullerene crystallization?  
 (b) Estimate the binding energy between two  $C_{60}$  molecules with a separation distance of 2 nm.  
 (c) Do you expect the binding energy to be smaller or larger for two molecules of  $C_{70}$ ? Briefly explain your answer.
- 1.19** Stable dispersions of  $C_{60}$  in water can be obtained by modifying the  $C_{60}$  surface with negative charges. Calculate the surface charge required to separate two  $C_{60}$  molecules by a distance of 5 nm.
- 1.20** Films composed of crystallized  $C_{60}$  can be intercalated with  $Li^+$  to serve as anodes for lithium-ion batteries.  $Li^+$  ions have a radius of 6 Å. The diameter



of  $C_{60}$  is 0.71 nm and the Lennard-Jones potential constants are  $A = 20 \text{ eV } \text{\AA}^6$  and  $B = 34.8 \times 10^3 \text{ eV } \text{\AA}^{12}$ .

- (a) Determine whether there is volume expansion in crystallized  $C_{60}$  when a  $\text{Li}^+$  ion occupies the space between two  $C_{60}$  molecules.
- (b) The Hamaker constant for crystallized  $C_{60}$  is  $4.02 \times 10^{-21} \text{ J}$ . How do you expect the binding energy of solid  $C_{60}$  to change when  $\text{Li}^+$  ions are introduced into the crystal? Briefly explain.

